Dilepton production from a nonequilibrium quark-gluon plasma in ultrarelativistic nucleus-nucleus collisions

M. Asakawa
*Center for Theoretical Physics, Laboratory for Nuclear Science and Department of Physics, Massachusetts Institute of Technology, Cambridge, Massachusetts 02139 and Department of Physics, Faculty of Science, University of Tokyo, Tokyo 113, Japan**

T. Matsui
Center for Theoretical Physics, Laboratory for Nuclear Science and Department of Physics, Massachusetts Institute of Technology, Cambridge, Massachusetts 02139
(Received 8 November 1990)

Dilepton production from a nonequilibrium quark-gluon plasma produced in ultrarelativistic nucleus-nucleus collisions is studied, based on the flux-tube model which has been formulated in terms of a model relativistic Boltzmann-Vlasov equation with a boost-invariant particle source term. This model kinetic equation is solved with the collision term in the relaxation-time approximation. In the collisionless limit, the solution of the kinetic equation becomes oscillatory, indicating the spontaneous excitation of the plasma oscillation. We study how such a nonequilibrium evolution of the system is reflected in the dilepton spectrum. It is shown that the dileptons emitted during such a nonequilibrium stage of matter evolution does not necessarily lead to a spectrum which interpolates smoothly the spectrum from thermal emission and that from the Drell-Yan mechanism. Our results show, on the contrary, that the dilepton spectrum is softened significantly in the absence of thermalization. M_T scaling, which is expected in scaling one-dimensional hydrodynamic evolution, is also broken due to the anisotropy in the phase-space distribution of quarks.

I. INTRODUCTION

Dilepton emission from the quark-gluon plasma produced in ultrarelativistic nucleus-nucleus collisions has been studied by numerous authors.[1-7] One of the most appealing points of dileptons as a probe of quark-gluon plasma is that leptons do not suffer strong final-state interactions; therefore, once created in the interior of the plasma, they will almost freely escape from the system carrying the information on the interior condition of produced matter. In contrast, hadrons are created only at the surface of the plasma, and their subsequent motion would be disturbed strongly by their mutual interactions until the matter is sufficiently diluted. Dileptons can also be used to study the production of various neutral vector mesons which are seen as resonance peaks in the dilepton invariant-mass spectrum. The change of the production rate of large-mass resonances, such as J/ψ, may also provide valuable information about the influence of the deconfining plasma medium on the production process.[8]

The standard procedure to estimate the expected yield of dileptons from the quark-gluon plasma is to assume local thermodynamic equilibrium for the phase-space distribution of the plasma consistuents, namely, quarks and gluons. This gives a simple formula for the differential emission rate of a dilepton with four-momentum q^μ per unit volume due to quark-antiquark annihilation: In the limit of vanishing quark and lepton masses,

$$\frac{d^4r}{d^4q} = \frac{R\alpha^2}{12\pi^4} e^{-q\cdot u/T}, \tag{1.1}$$

where α is the QED fine-structure constant, $R=\sum e_f^2$ is the color and flavor sum of the square of fractional quark charges, and u^μ and T are local flow vector and temperature, respectively. The total yield of dileptons can be obtained by integrating (1.1) over the space-time region occupied by the thermalized plasma, taking into account the variation of local temperature and flow as determined by solving hydrodynamic equations.

It is known, however, that the result of such calculations depends strongly on the initial conditions of the hydrodynamic evolution of the plasma. For example, the thermal dileptons in the large-mass region (>2 GeV) are dominated by those produced at the hottest stage of plasma: The falloff of the yield at large masses is essentially determined by the "Boltzmann factor" e^{-M/T_0}, where T_0 is the "initial" temperature of the plasma, and the prefactor is determined by the "initial" volume occupied by the plasma, which is given, according to Bjorken's boost-invariant hydrodynamic expansion,[9] by $V_0 \propto \pi R^2 \tau_0$, where τ_0 is the proper time when the boost-invariant hydrodynamic expansion starts. It is important to emphasize here that the term "initial" only loosely refers to the time when thermalization of plasma is achieved; it does not mean that the plasma is created instantaneously at this time or that there is no source of dilepton before this time. On the contrary, it is commonly expected that the high-mass dileptons are dominated by the Drell-Yan process, namely, the annihilation of quark and antiquark contained in the colliding nuclei, which operates at the very beginning of the collision, loosely speaking, when

two Lorentz-contracted nuclei overlap. Thermalization of the plasma is expected to take place sometime after this, and the transient period between these two distinct space-time regions, which may be referred to as the preequilibrium regime, may also give a source of dileptons. The result of the thermal dilepton emission calculation quoted above therefore clearly indicates the importance of the preequilibrium stage of the plasma evolution for dilepton emission. One would naively expect that the inclusion of such a nonequilibrium plasma process would interpolate the spectrum from the Drell-Yan process and that from the thermalized plasma.[5]

Despite its obvious importance, so far there have been only very few attempts to calculate the dilepton emission from a nonequilibrium plasma. This is largely due to the difficulty in describing the nonequilibrium evolution of matter produced in the collision: For such a description it is essential to incorporate the mechanism of matter formation. Białas and Blaizot[10] calculated dilepton emission using the model of an oscillating quark-antiquark plasma which had been studied earlier by Białas and Czyż.[11] This model describes the collisionless evolution of a system of quarks and antiquarks interacting with a classical color field in terms of a relativistic Boltzmann-Vlasov equation which conserves the particle number. The boost-invariant initial conditions for the particle distribution in phase space were set at certain early proper time, as was done in the hydrodynamic model of Bjorken. Therefore, this model still lacks the description of the formation stage of such plasma.

In this paper we study dilepton emission from a quark-gluon plasma, based on the flux-tube model for ultrarelativistic nucleus-nucleus collisions.[12–15] This model assumes that two Lorentz-contracted nuclei get color charged when they pass through each other by multiple soft gluon exchange. The strong color field which spans between the two receding color charged nuclei will decay by pair creation (Schwinger mechanism[16–18]), creating a quark-gluon plasma in the flux tube. This picture is a natural extension of the Low-Nussinov model for the hadronic interactions.[19,20] The expansion of the plasma created in this way has been described by using the model Boltzmann equation with a boost-invariant source term,[21] which was later extended to include the Vlasov term in an Abelian approximation for the color charge and solved by taking the hydrodynamic limit for the cylindrical expansion.[22] In this work we construct the solution for this model transport equation without taking the hydrodynamic limit, and the result is used to calculate the dilepton emission spectrum.

An important new feature that arises in the evolution of the plasma in the absence of collision is the excitation of collective plasma oscillation. Usually, plasma oscillations are treated based on the linearized Boltzmann-Vlasov equation for the small perturbation of the system in thermodynamic equilibrium. Białas and Czyż[11] showed, based on specific initial conditions, that such a collective plasma oscillation can be excited in the boost-invariant fashion. This result was confirmed later by Białas and co-workers,[23] based on a model which is similar to ours, but also incorporates the non-Abelian nature of the color charge,[24,25] and by Banerjee, Bhalero, and Ravishankar,[26] based on a model similar to ours. We shall show in this paper that collective plasma oscillation is almost always excited spontaneously, irrespective of the choice of specific initial conditions, in the collisionless plasmas which undergo a boost-invariant longitudinal expansion. Our major concern in this paper is how such nonequilibrium nontrivial evolution of the plasma is reflected in the dilepton spectrum.

We will show that such nonequilibrium plasma evolution with a collective plasma oscillation will yield more low-mass dileptons compared with the equilibrium plasma evolution which results in a similar final state for the global observables, such as the energy per unit rapidity; at the high-mass region our model gives a Gaussian-shape spectrum and therefore does not lead to the spectrum which interpolates the power-law behavior of the Drell-Yan process and the exponential behavior of the thermal pairs. M_T scaling, which has been predicted earlier based on the boost-invariant equilibrium evolution model,[4] is violated in this model in a way opposite to the violation due to the transverse expansion.[6]

The rest of this paper is organized as follows: In the next section we derive the basic formula for dilepton emission from a nonequilibrium plasma based on the kinetic theory. This is just a straightforward generalization of the calculation of the thermal dilepton emission from quark-gluon plasma. The results of this section can be applicable for any model for nonequilibrium evolution of the plasma. In Sec. III, we describe a model kinetic theory which describes a nonequilibrium space-time evolution of the quark-gluon plasma based on the flux-tube model. We examine the collisionless limit of our model kinetic equation in Sec. IV in the linear approximation and show how plasma oscillation will show up in the boost-invariant nonequilibrium evolution of the system. Our numerical results are presented and discussed in Sec. V. A short summary and conclusions are given in Sec. VI.

II. KINETIC THEORY FOR DILEPTON PRODUCTION

In this section we discuss the basic method to compute the dilepton emission from a quark-gluon plasma based on the kinetic theory. The one-particle distribution function plays the central role in such calculation. The one-body distribution function $f_i(x;\mathbf{p})$ is defined so that

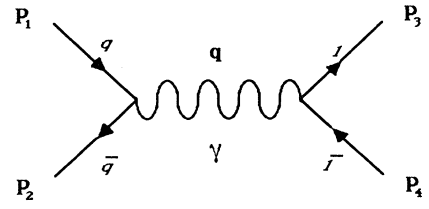

FIG. 1. Lowest-order diagram for $q\bar{q}\to l\bar{l}$.

$f_i(x,\mathbf{p})d^3\mathbf{x}\,d^3\mathbf{p}$ gives the number of particles of species i (spin, color, flavor) in a small phase-space element $d^3\mathbf{x}\,d^3\mathbf{p}$ at time t. In the absence of many-body correlation in the system,, which is the condition usually assumed to construct the Boltzmann collision term, the local emission rate of a dilepton by the annihilation of a pair of quark and antiquark is given in terms of the one-particle distribution function as

$$r(x)\equiv\frac{d^4N}{d^4x}$$
$$=\sum_i\int\frac{d^3p_1}{(2\pi)^3 2E_1}\int\frac{d^3p_2}{(2\pi)^3 2E_2}\int\frac{d^3p_3}{(2\pi)^3 2E_3}\int\frac{d^3p_4}{(2\pi)^3 2E_4}$$
$$\times f_i(x;\mathbf{p}_1)\bar{f}_i(x;\mathbf{p}_2)|\mathcal{M}(q_i\bar{q}_i\to l\bar{l})|^2(2\pi)^4\delta^4(p_1+p_2-p_3-p_4)\ , \tag{2.1}$$

where $p_i^\mu=(E_i,\mathbf{p}_i)$ are the four-momentum of the quark and antiquark ($i=1,2$) and lepton pair ($i=3,4$), and $\mathcal{M}(q_i\bar{q}_i\to l\bar{l})$ is the invariant matrix element for the process under consideration. Here the summation is taken over the initial quark spin, color, and flavor, and the final lepton spin as well. This formula generalizes the formula (1.1) for the emission rate from thermalized plasma into situations where thermodynamic equilibrium is not established in plasma.

A. Emission rate in lowest order

We now compute the dilepton emission rate in the lowest-order $O(\alpha^1\alpha_s^0)$ with respect to the QED and QCD couplings. The corresponding Feynman diagram for the process is shown in Fig. 1. As is well known, the sum over the initial quark and final lepton spins of the square of this matrix element is given by

$$\sum_{\text{spin}}|\mathcal{M}(q_i\bar{q}_i\to l\bar{l})|^2=\frac{e^4}{q^4}e_i^2 h_{\mu\nu}l^{\mu\nu}\ , \tag{2.2}$$

where

$$h^{\mu\nu}=4[(p_1\cdot p_2+m_q^2)g^{\mu\nu}-p_1^\mu p_2^\nu-p_1^\nu p_2^\mu]\ , \tag{2.3}$$

$$l^{\mu\nu}=4[(p_3\cdot p_4+m_l^2)g^{\mu\nu}-p_3^\mu p_4^\nu-p_3^\nu p_4^\mu]\ , \tag{2.4}$$

where m_q and m_l are the mass of quarks and leptons, respectively, and e_i is the fractional quark charge: $e_u=\frac{2}{3}$, $e_d=-\frac{1}{3},\ldots$ [Throughout this paper we use the metric tensor $g^{\mu\nu}=\text{diag}(1,-1,-1,-1)$.] This formula allows us to compute the phase-space integrals for quarks and leptons separately.

$$r(x)=\int d^4q\frac{\alpha^2}{\pi^2}\frac{1}{M^4}W^{\mu\nu}(x,q)L_{\mu\nu}(q)\ , \tag{2.5}$$

where

$$W_{\mu\nu}(x,q)=\sum_{\text{color,flavor}}e_i^2\int\frac{d^3p_1}{(2\pi)^3 2E_1}\int\frac{d^3p_2}{(2\pi)^3 2E_2}f_i(x;p_1)\bar{f}_i(x;p_2)h_{\mu\nu}(2\pi)^4\delta^4(p_1+p_2-q)\ , \tag{2.6}$$

$$L_{\mu\nu}(q)=\int\frac{d^3p_3}{(2\pi)^3 2E_3}\int\frac{d^3p_4}{(2\pi)^3 2E_4}l_{\mu\nu}(2\pi)^4\delta^4(p_3+p_4-q)\ . \tag{2.7}$$

The phase-space integral of the leptonic tensor $L_{\mu\nu}$ can be evaluated easily:

$$L^{\mu\nu}(q)=\left[g^{\mu\nu}-\frac{q^\mu q^\nu}{q^2}\right]\frac{M^2}{6\pi^2}\left[1-\frac{4m_l^2}{M^2}\right]^{1/2}\left[1+\frac{2m_l^2}{M^2}\right]\theta\left[1-\frac{4m_l^2}{M^2}\right]\ . \tag{2.8}$$

Inserting (2.8) into (2.5) and using $q_\mu W^{\mu\nu}=0$, because of the current conservation, we find the following formula for the differential dilepton emission rate per unit volume:

$$\frac{d^4r}{d^4q}=\frac{\alpha^2}{6\pi^2}\frac{1}{M^2}F(m_l/M)W_\mu{}^\mu(x,q)\ , \tag{2.9}$$

where we have introduced the function $F(x)=(1+2x^2)(1-4x^2)^{1/2}\theta(1-4x^2)$ to denote the kinematical factor due to the finite lepton mass.

The thermal emission rate (1.1) can be derived from this formula by inserting the equilibrium one-particle distribution function approximated by the Boltzmann form $f_{\rm eq}(x,p)=\exp[-p\cdot u(x)/T(x)]$ into (2.6):

$$W^{\mu\nu}_{\rm eq}(x,q)=\left[g^{\mu\nu}-\frac{q^\mu q^\nu}{q^2}\right]R\frac{M^2}{6\pi^2}e^{-q\cdot u/T}, \tag{2.10}$$

where $R=N_c\sum_{i=u,d}e_i^2=3\times(\frac{1}{9}+\frac{4}{9})=\frac{5}{3}$. Inserting this into (2.9), we find

$$\frac{d^4r}{d^4q}=\frac{R\alpha^2}{12\pi^4}e^{-q\cdot u/T}F(m_l/M), \tag{2.11}$$

which coincides with (1.1) when $M\gg m_l$ since $F(x)=1$ for $x\ll 1$. The formula (2.9) with (2.6) is therefore the generalization of (1.1) for an arbitrary form of one-particle distribution function.

The total yield of dileptons emitted from a plasma produced by a single collision event can be calculated by integrating the local production rate (2.9) over the entire four-volume occupied by the plasma,

$$\begin{aligned}\frac{d^4N}{dM_T^2\,dy\,d^2q_T}&=\frac{1}{2}\int d^4x\frac{d^4r}{d^4q}\\&=\frac{\alpha^2}{12\pi^2}\frac{1}{M^2}F(m_l/M)\int d^4x\,W(x,q),\end{aligned} \tag{2.12}$$

where we have used $d^4q=\frac{1}{2}dM_T^2\,dy\,d^2q_T$ and introduced a compact notation for the trace of $W^{\mu\nu}$,

$$\begin{aligned}W(x,q)&\equiv W_\mu{}^\mu(x,q)\\&=\frac{M^2}{\pi^2}\sum_{\text{color,flavor}}e_i^2\int\frac{d^3p_1}{2E_1}\int\frac{d^3p_2}{2E_2}f_i(x;p_1)\bar f_i(x;p_2)\delta^4(p_1+p_2-q).\end{aligned} \tag{2.13}$$

B. Formula for boost-invariant distributions

One can reduce the multidimensional integral in (2.12) to a simpler one by using the symmetry of the distribution functions. Let us assume here, along with Bjorken,[9] that at sufficiently high energies the evolution of the central rapidity region is approximately invariant under the Lorentz boost in the beam (longitudinal) direction. If we further assume the transverse uniformity of the system, this implies[21,27] that the one-body distribution function is a function only of three independent variables τ, p_T, and $\xi=\eta-y$, defined by

$$\begin{aligned}&\tau=(t^2-z^2)^{1/2},\quad \eta=\frac{1}{2}\ln\left[\frac{t+z}{t-z}\right],\\&p_T=(E^2-p_L^2)^{1/2},\quad y=\frac{1}{2}\ln\left[\frac{E+p_L}{E-p_L}\right].\end{aligned} \tag{2.14}$$

For example, in the case of equilibrium plasma which undergoes boost-invariant one-dimensional scaling hydrodynamic expansion, $u^\mu=(\cosh\eta,0,0,\sinh\eta)$, insertion of (2.11) with $q\cdot u=M_T\cosh(\eta-y)$ into (2.12) gives

$$\begin{aligned}\frac{d^4N}{dM_T^2\,dy\,d^2q_T}&=\frac{R\alpha^2}{24\pi^3}F(m_l/M)\int d^4x\,e^{-M_T\cosh(\eta-y)/T(\tau)}\\&=\frac{R\alpha^2}{24\pi^3}F(m_l/M)\int d^2\mathbf{r}_\perp d\tau\,\tau 2K_0(M_T/T(\tau)),\end{aligned} \tag{2.15}$$

where $K_0(x)$ is the modified Bessel function of order 0 and $\mathbf{r}_\perp=(x,y)$ is the transverse coordinates. This formula predicts that for $M\gg m_l$, where $F(m_l/M)\simeq 1$, the thermal dilepton yield does not depend on two variables M and q_T separately, but only on $M_T=(M^2+q_T^2)^{1/2}$. This M_T scaling is a well-known consequence of the one-dimensional scaling hydrodynamic expansion of plasma.[4] It is also known, however, that this M_T scaling is violated in the presence of the transverse expansion.[6] This scaling is also violated in the case of nonequilibrium plasma evolution, even in the absence of transverse expansion, as we shall see below.

In more general cases of boost-invariant nonequilibrium distribution, the scalar function $W(x,q)$ becomes a function only of four independent variables: τ, M, q_T, and $\eta-y$. Then, by inserting (2.13) into (2.12) and writing the space-time integral in terms of the light-cone variables $d^4x=d^2\mathbf{r}_\perp\tau\,d\tau\,d\eta$,

$$\frac{d^4N}{dM_T^2\,dy\,d^2q_T}=\frac{\alpha^2}{12\pi^2}\frac{1}{M^2}F(m_l/M)S\int\tau\,d\tau\int_{-\infty}^{\infty}d\eta\,W(\tau,M,q_T,\eta-y), \tag{2.16}$$

where $S=\int d^2\mathbf{r}_\perp$ is the transverse cross section of the plasma. We can immediately see that the final result should depend only on two variables M and q_T, but not on y. This is a direct consequence of the longitudinal boost invariance of the system. We show in Appendix A that $W(\tau,M,q_T,\xi)$ is given by the following double integral of quark and antiquark distribution functions:

$$W(\tau,M,q_T,\xi)=\frac{RM^2}{2\pi^2}\int_{-\infty}^{\infty}d\xi_1\int_{p_-}^{p_+}dp_{T_1}\frac{p_{T_1}f(\tau,p_{T_1},\xi_1)\bar{f}(\tau,p_{T_2},\xi_2)}{\{p_{T_1}^2q_T^2-[p_{T_1}M_T\cosh(\xi-\xi_1)-M^2/2]^2\}^{1/2}}\ , \tag{2.17}$$

where the arguments of the antiquark distribution function are related to the integration variables by

$$p_{T_2}=(M_T^2-2M_Tp_{T_1}\cosh\xi_1+p_{T_1}^2)^{1/2}\ , \tag{2.18}$$

$$\sinh\xi_2=\frac{M_T\sinh\xi-p_{T_1}\sinh\xi_1}{(M_T^2-2M_Tp_{T_1}\cosh\xi_1+p_{T_1}^2)^{1/2}}\ , \tag{2.19}$$

and the upper and lower bounds of the p_T integral are given by

$$p_\pm=\frac{M^2/2}{M_T\cosh(\xi-\xi_1)\mp q_T}\ . \tag{2.20}$$

The remaining four-dimensional integration needs to be performed by numerical computation for a given one-body distribution function.

III. FLUX-TUBE MODEL FOR NONEQUILIBRIUM PLASMA EVOLUTION

As we have seen in the previous section, the quark (antiquark) one-body distribution function is the key object which we need to obtain in order to estimate the dilepton emission rate. In this section we formulate and discuss a model transport theory based on the flux-tube model which describes the nonequilibrium evolution of a quark-gluon plasma in terms of the quark one-body distribution function.

A. Model kinetic theory

Let us first summarize briefly our basic picture for the plasma evolution in the flux-tube model. We consider central collision of two heavy nuclei at extreme high energies: The velocity of nuclei can therefore be taken as that of light; the colliding nuclei are highly Lorentz contracted so that they appear as infinitesimally thin plates. In our semiclassical formulation we shall neglect the intrinsic longitudinal extension of the Lorentz-contracted nuclear wave function due to the wee components.[28] Two plates collide at $t=z=0$ over some extended area in the transverse (x,y) direction. At the moment of the collision, two plates are color charged by random gluon exchange. Nuclei thus form color capacitor plates after the collision. The region between them is filled with strong color field. This strong color field will immediately begin to polarize the vacuum, creating quark-antiquark pairs and gluon pairs by quantum tunneling. This tunneling rate has been computed by Schwinger[16] and others[17,18] using the proper time method for QED and by Casher, Neuberger, and Nussinov[29] and others[30–32] by the WKB method, and these results have been applied to the pair creation in the color flux tube.

The quarks, antiquarks, and gluons created by tunneling from the coherent color field will suffer two types of interaction: collisions among themselves and the interaction with the remaining color field. Collisions among the excitations will change the phase-space distribution of them and drive it toward the form in (local) thermodynamic equilibrium, while the interaction with the remaining field will accelerate those charged particles into two opposite directions parallel to the field, depending on the charge of each constituent. The latter process will generate a conductive color current in the system and cause color separation in the plasma.

All these effects in the plasma evolution may be studied in terms of the following model Boltzmann-Vlasov equation:[21,22]

$$p^\mu\partial_\mu f_i-gp^\mu F_{\mu\nu}\frac{\partial f_i}{\partial p_\nu}=C_i+S_i\ , \tag{3.1}$$

$$p^\mu\partial_\mu \bar{f}_i+gp^\mu F_{\mu\nu}\frac{\partial \bar{f}_i}{\partial p_\nu}=\bar{C}_i+\bar{S}_i\ , \tag{3.2}$$

where f_i ($\bar{f}_i$) is the distribution function of the quarks (antiquarks) (i represents the spin, color, and flavor states), g is the effective coupling constant between the quarks and the background color field, C_i ($\bar{C}_i$) is the collision term, and S_i ($\bar{S}_i$) is the source term which represents the $q\bar{q}$ pair creation by the external field. In this paper we approximate the color field as an Abelian one, although the non-Abelian nature of the color field might cause some interesting effects. We shall also neglect the gluon degrees of freedom entirely in the rest of our calculation just for simplicity. The extension to include gluon excitations taking into account non-Abelian nature of the color charge may be performed along the line of Ref. 23.

We note that in the above covariant expression of the Vlasov term the four components of the momentum p are treated as if they were all independent variables, although actually only three spatial momentum components are in-

dependent because of the on-shell condition $p^2=m^2$. It is understood that $f(x;p)=f(x;\mathbf{p},E(\mathbf{p}))$.

The collision terms are usually written as the phase-space integral of the distribution function similar to (2.1).[33] Here we take the following simplified relaxation-time approximation for the collision term:[27]

$$C_i=-\frac{p^\mu u_\mu(f_i-f_i^{\rm eq})}{\tau_c}\ ,\qquad \bar{C}_i=-\frac{p^\mu u_\mu(\bar{f}_i-f_i^{\rm eq})}{\tau_c}\ , \tag{3.3}$$

where

$$f_i^{\rm eq}=\frac{1}{\exp(p_\mu u^\mu/T)+1} \tag{3.4}$$

is the equilibrium distribution function characterized by local flow vector $u^\mu=\gamma(1,\mathbf{v})$ with $\gamma=1/(1-\mathbf{v}^2)^{1/2}$ and local temperature $T(x)$. It should be understood here that the temperature $T(x)$ is only a parameter which characterises the collision term: The actual state of the system is described by the distribution function $f_i(x;p)$ not by $f_i^{\rm eq}(x;p)$. We shall later discuss the condition which determines the time evolution of $T(x)$. We have neglected the possible i dependence of the relaxation time τ_c in the above parametrization.

The source term has been constructed in Ref. 22 for the case that the field tensor can be written as

$$F^{\mu\nu}=\mathcal{E}(s^\mu t^\nu-s^\nu t^\mu)\ , \tag{3.5}$$

where s^μ and t^μ are unit spacelike and timelike vectors, respectively, which satisfy $-s^2=t^2=1$ and $s\cdot t=0$. In this case one can find a local Lorentz frame where the field tensor contains only an electric-field component with the strength $\mathcal{E}$ and no magnetic field. In the following calculation we assume the transverse uniformity of the system and take the following simple form for the field tensor:

$$F_{03}=-F_{30}=\mathcal{E}\quad\text{and}\quad F_{\mu\nu}=0\ , \tag{3.6}$$

for $(\mu,\nu)\neq(0,3)$ or (3,0). We note that this form of the field tensor is invariant under the Lorentz boost in the longitudinal direction, namely, z direction, and this symmetry should be reflected in the form of the source term. Using the light-cone coordinate (2.14), we write the source term as

$$S_i(x,p)=\bar{S}_i(x,p)=-g|\mathcal{E}(\tau)|\ln\left[1-\exp\left[-\frac{\pi p_T^2}{g|\mathcal{E}(\tau)|}\right]\right]\delta(\eta-y)$$
$$\simeq g|\mathcal{E}(\tau)|\exp\left[-\frac{\pi p_T^2}{g|\mathcal{E}(\tau)|}\right]\delta(\eta-y)\ . \tag{3.7}$$

A few more comments on this form of the source term are in order. The p_T dependence has been taken from the well-known result of the differential pair-creation rate obtained by the WKB method.[29] The longitudinal momentum dependence, which cannot be determined by the pair-creation calculation, has been taken so that the longitudinal velocity of the particle satisfies the scaling relation $v_z=z/t$ at the time of the creation. This scaling relation is written as $\eta=y$ in our coordinate system. The normalization of the source term is determined so that the integrated particle production rate coincides with Schwinger's formula for the pair-creation rate. In the above expression it is shown explicitly that the electric-field strength depends on the proper time. This is because the field strength attenuates as a result of the transfer of the field energy to the particle kinetic energy by the pair creation and also by particle acceleration. The time evolution of the field strength can be determined by the conservation of the total energy in the system, as we shall see later. We have also explicitly indicated possible i dependence of the source term through that of the quark mass. Hereafter we consider the simple case of two massless flavors (up and down quarks) and therefore set $m_i=0$.

As the initial condition for the distribution function, we impose

$$f_i(x;p)=0,\quad \bar{f}_i(x;p)=0,\quad \mathcal{E}(\tau)=\mathcal{E}_0\ \text{ at }\tau=0\ , \tag{3.8}$$

which implies that all particles are produced by the source term from the field. It is obvious that these initial conditions are invariant under the Lorentz boost in the longitudinal direction and the translation in the transverse direction. Therefore, it follows from the same symmetries in the source term (3.7) that the solution of the transport equation must possess these symmetries and that the distribution functions are written as functions of only three variables τ, p_T, and $\xi=\eta-y$. The distribution functions also do not depend on the quark flavor for the same reason. Therefore, we can write

$$f_i(x;p)=f(\tau,p_T,\xi),\quad \bar{f}_i(x;p)=\bar{f}(\tau,p_T,\xi)\ . \tag{3.9}$$

With these symmetries in the solution, we can reduce the kinetic equations (3.1) and (3.2) to

$$\frac{\partial f}{\partial\tau}-\left[\frac{\tanh\xi}{\tau}+\frac{g\mathcal{E}}{p_T\cosh\xi}\right]\frac{\partial f}{\partial\xi}=-\frac{f-f_{\rm eq}}{\tau_c}+\frac{S}{p_T\cosh\xi} \tag{3.10}$$

and

$$\frac{\partial \bar{f}}{\partial \tau}-\left[\frac{\tanh\xi}{\tau}-\frac{g\mathcal{E}}{p_T\cosh\xi}\right]\frac{\partial \bar{f}}{\partial \xi}=-\frac{\bar{f}-f_{\rm eq}}{\tau_c}+\frac{S}{p_T\cosh\xi}\ , \tag{3.11}$$

where the equilibrium distribution function is understood also to possess the symmetries of the solution and is therefore written as

$$f_{\rm eq}(\tau,p_T,\xi)=\frac{1}{\exp[p_T\cosh\xi/T(\tau)]+1}\ , \tag{3.12}$$

and we have used the following scaling form for the flow velocity:

$$u^\mu=(\cosh\eta,0,0,\sinh\eta)\ . \tag{3.13}$$

Note that (3.11) for the antiquark distribution function can be obtained from (3.10) by the "charge-conjugation" operation $\xi\rightarrow-\xi$. Since the same initial conditions are taken for f and $\bar{f}$, this implies the following symmetry:

$$f(\tau,p_T,\xi)=\bar{f}(\tau,p_T,-\xi)\ . \tag{3.14}$$

Therefore, once we find the solution for the quark distribution function f by solving (3.10), the antiquark distribution function $\bar{f}$ can be immediately obtained from (3.14). This symmetry relation will be used very often in the following calculation.

We still have to show how to determine the time evolution of the temperature $T(\tau)$ contained in the collision term (3.3) and that of the field strength $\mathcal{E}(\tau)$, which appears both in the source term (3.7) and the Vlasov term. The relations which determine these quantities are obtained from the energy-momentum conservation law as follows. To show this we first take the moment of the kinetic equations (3.1) and (3.2),

$$\partial_\mu T_q^{\mu\nu}-g\int d\Gamma\, p^\mu p^\nu F_{\mu\lambda}\frac{\partial f}{\partial p_\lambda}=\int d\Gamma\, p^\nu C+\int d\Gamma\, p^\nu S \tag{3.15}$$

and

$$\partial_\mu T_{\bar{q}}^{\mu\nu}+g\int d\Gamma\, p^\mu p^\nu F_{\mu\lambda}\frac{\partial \bar{f}}{\partial p_\lambda}=\int d\Gamma\, p^\nu \bar{C}+\int d\Gamma\, p^\nu S\ , \tag{3.16}$$

where

$$T_q^{\mu\nu}=\sum_i\int\frac{d^3p}{(2\pi)^3E}p^\mu p^\nu f_i=\int d\Gamma\, p^\mu p^\nu f$$

and

$$T_{\bar{q}}^{\mu\nu}=\int d\Gamma\, p^\mu p^\nu \bar{f} \tag{3.17}$$

are the kinetic energy-momentum tensors of the quarks and antiquarks, respectively. In the above expression we have used a shorthand notation for the invariant phase-space volume element:

$$d\Gamma=\frac{\gamma\, d^3p}{(2\pi)^3E}=\frac{\gamma p_T\, dp_T\, d\xi}{(2\pi)^2}\ , \tag{3.18}$$

where $\gamma=2\times3\times2=12$ is the spin, color, and flavor degrees of freedom for quarks. Equations (3.15) and (3.16) express the energy-momentum conservation for quarks and antiquarks, respectively. Since the energy and momentum are conserved in each collision, the moment of the sum of the collision term should vanish:

$$\int d\Gamma\, p^\nu C+\int d\Gamma\, p^\nu \bar{C}=0\ . \tag{3.19}$$

Inserting $C=-(p_\mu u^\mu)(f-f^{\rm eq})/\tau_c$ and $\bar{C}=-(p_\mu u^\mu)(\bar{f}-f^{\rm eq})/\tau_c$, taking the contraction with u_ν, and using $p_\mu u^\mu=p_T\cosh\xi$, we find the following relation between the proper energy density, $e(\tau)\equiv u_\mu u_\nu(T_q^{\mu\nu}+T_{\bar{q}}^{\mu\nu})$ and the temperature:

$$e(\tau)=\int d\Gamma(p_T\cosh\xi)^2(f+\bar{f})=\frac{7\gamma\pi^2}{120}T(\tau)^4\ . \tag{3.20}$$

This is the equation which determines the time dependence of the temperature parameter in the collision term.

The equation which determines the time evolution of the field strength can be found from the total energy-momentum conservation,

$$\partial_\mu T_q^{\mu\nu}+\partial_\mu T_{\bar{q}}^{\mu\nu}+\partial_\mu T_f^{\mu\nu}=0\ , \tag{3.21}$$

where $T_f^{\mu\nu}=\mathrm{diag}(\mathcal{E}^2/2,\mathcal{E}^2/2,\mathcal{E}^2/2,-\mathcal{E}^2/2)$ is the energy-momentum tensor of the field. Using (3.6), (3.7), (3.15), and (3.16), we can reduce this relation to

$$\frac{d\mathcal{E}}{d\tau}=-2a\ \mathrm{sgn}(\mathcal{E})|\mathcal{E}|^{3/2}+g\int d\Gamma\, p_T\sinh\xi(f-\bar{f})\ , \tag{3.22}$$

where $a=\gamma g^{5/2}/(16\pi^3)$. This equation determines the time evolution of the color field strength.

Equations (3.10), (3.14), (3.20), and (3.22) form a closed set of equations which determine the time evolution of f, $\bar{f}$, T, and $\mathcal{E}$ with given initial conditions.

B. Scaling of the solutions

In the collisionless limit our model has only one dimensional parameter, the initial field strength $\mathcal{E}_0$, which has the dimension of (energy)^2 or, equivalently, (time)$^{-2}$ in natural units. Thus it is easy to see the dependence of dimensionful quantities on $\mathcal{E}_0$: It can be determined by dimensional analysis.[15] For example, the time scale which characterizes the time evolution of the system is inversely proportional to $\mathcal{E}_0^{1/2}$ and the average momentum of the quarks must scale in proportion to $\mathcal{E}_0^{1/2}$. Our equations contain two more dimensionless parameters, the coupling between the quarks and color field g and the effective quark degrees of freedom γ. We discuss in the rest of this section how the solutions of our model kinetic equa-

tion may depend on these parameters as well as $\mathcal{E}_0$.

For this purpose we write down once again the closed set of equations which determine the time evolution of the system:

$$\frac{\partial f}{\partial \tau}-\left[\frac{\tanh\xi}{\tau}+\frac{g\mathcal{E}}{p_T\cosh\xi}\right]\frac{\partial f}{\partial \xi} =-\frac{f-f_{\rm eq}}{\tau_c}+\frac{g|\mathcal{E}|\exp(-\pi p_T^2/g|\mathcal{E}|)\delta(\xi)}{p_T\cosh\xi}\ , \tag{3.23}$$

$$\frac{d\mathcal{E}}{d\tau}=-\frac{g^{5/2}\gamma}{8\pi^3}\mathrm{sgn}(\mathcal{E})|\mathcal{E}|^{3/2}+g\int d\Gamma\, p_T\sinh\xi(f-\bar f)\ , \tag{3.24}$$

$$\frac{7\gamma\pi^2}{120}T^4=\int d\Gamma(p_T\cosh\xi)^2(f+\bar f)\ . \tag{3.25}$$

The last equation for the temperature is not a dynamical equation, but is just a subsidiary condition to determine $T(\tau)$ in the equilibrium distribution (3.12), which appears in the first kinetic equation.

To motivate ourselves to find a natural way to scale the variables, let us first take a look at the kinetic equation. We immediately notice that the electric-field strength $\mathcal{E}$ appears in the kinetic equation always in the specific combination with the coupling constant as $g\mathcal{E}$, which is just the strength of the Lorentz force acting on the quarks. This suggests that the natural time scale which characterizes the time evolution of the distribution function would be

$$\tau_{\rm k}=(g\mathcal{E}_0)^{-1/2}\ , \tag{3.26}$$

and that the natural energy-momentum scale of quarks would be the reciprocal of this time scale. In fact, if we introduce the new dimensionless variables

$$\hat\tau=(g\mathcal{E}_0)^{1/2}\tau,\quad \hat p_T=(g\mathcal{E}_0)^{-1/2}p_T\ , \tag{3.27}$$

and write

$$\begin{aligned}&\hat f(\hat\tau,\hat p_T,\xi)=f(\tau,p_T,\xi)\ ,\\ &\hat{\bar f}(\hat\tau,\hat p_T,\xi)=\bar f(\tau,p_T,\xi)\ ,\\ &\hat f_{\rm eq}(\hat t,\hat p_T,\xi)=f_{\rm eq}(\tau,p_T,\xi)\ ,\\ &\hat T(\hat\tau)=(g\mathcal{E}_0)^{-1/2}T(\tau)\ ,\\ &\hat{\mathcal{E}}(\hat\tau)=\mathcal{E}(\tau)/\mathcal{E}_0\ ,\end{aligned} \tag{3.28}$$

then, writing the phase-space integral explicitly with

$$d\Gamma=\gamma g\mathcal{E}_0\frac{\hat p_T\,d\hat p_T\,d\xi}{(2\pi)^2}\equiv\gamma g\mathcal{E}_0\,d\hat\Gamma\ , \tag{3.29}$$

we can reduce (3.10), (3.20), and (3.22) to

$$\frac{\partial \hat f}{\partial \hat t}-\left[\frac{\tanh\xi}{\hat\tau}+\frac{\hat{\mathcal{E}}}{\hat p_T\cosh\xi}\right]\frac{\partial \hat f}{\partial \xi} =-\frac{\hat f-\hat f_{\rm eq}}{\hat\tau_c}+\frac{|\hat{\mathcal{E}}|\exp(-\pi\hat p_T^{\,2}/|\hat{\mathcal{E}}|)\delta(\xi)}{\hat p_T\cosh\xi}\ , \tag{3.30}$$

$$\frac{d\hat{\mathcal{E}}}{d\hat\tau}=-\frac{g^2\gamma}{8\pi^3}\left[\mathrm{sgn}(\hat{\mathcal{E}})|\hat{\mathcal{E}}|^{3/2}-8\pi^3\int d\hat\Gamma\sinh\xi(\hat f-\hat{\bar f})\right]\ , \tag{3.31}$$

$$\frac{7\pi^2}{120}\hat T^4=\int d\hat\Gamma(\hat p_T\cosh\xi)^2(\hat f+\hat{\bar f})\ , \tag{3.32}$$

respectively, where we have rescaled the collision time by

$$\hat\tau_c=\tau_c/\tau_{\rm k}\ . \tag{3.33}$$

We have eliminated all parameters from the temperature equation (3.32) by the scaling (3.27) and (3.28). This is a rather trivial result since the temperature equation (3.32) does not depend on γ in any case and the momentum and temperature are measured using the same scale. More importantly, the scaled kinetic equation becomes parameter free in the collisionless limit $\tau_c\to\infty$ by this scaling. The parameters g and γ now appear only in the field equation in the specific combination $g^2\gamma$. We note that the absence of the parameter $g^2\gamma$ in the kinetic equation does not mean that the scaled distribution function is independent of this parameter. It still depends on $g^2\gamma$ because of the coupling to the field strength $\hat{\mathcal{E}}$, which apparently depends on this parameter.

There is yet another natural way to scale the variables. We may have chosen

$$\tau_0=\frac{16\pi^3}{g^{5/2}\gamma\mathcal{E}_0^{1/2}}=\frac{16\pi^3}{g^2\gamma}\tau_{\rm k}\ , \tag{3.34}$$

instead of (3.26), for the time scale, keeping the energy scale as before. If we adopted this scheme, then we would be able to eliminate all parameters from the field equation. In this case the parameter $g^2\gamma$ would appear in the rescaled kinetic equation, and therefore the time evolution of the rescaled field intensity would depend on the value of $g^2\gamma$ through its coupling to the rescaled distribution function. This choice is particularly convenient in the absence of the Vlasov term, since in this case the field equation does not contain the term which involves the distribution function and therefore can be immediately integrated, yielding[21]

$$\mathcal{E}(\tau)=\frac{\mathcal{E}_0}{(1+\tau/\tau_0)^2}\ . \tag{3.35}$$

We note that the leading behavior of $\mathcal{E}(\tau)$ for small τ/τ_0,

$$\mathcal{E}(\tau)=\mathcal{E}_0\left[1-\frac{2\tau}{\tau_0}+O((\tau/\tau_0)^2)\right]\ , \tag{3.36}$$

is unchanged even in the presence of the Vlasov term. This is so because the Vlasov term does not play an important role in determining the field evolution at very early times when the number of particles in the system is still very small.

C. Integral form of the kinetic equation

Our model Boltzmann-Vlasov equation [Eq. (3.10)] is not suitable in its original differential form for the numer-

ical integration since it contains a singular function $[\delta(\xi)]$ in the source term. We rewrite it here in an integral form by using the method of characteristics.

The essence of the method is to read the left-hand side of the partial differential equation (3.10) as a total derivative with respect to τ along the characteristic lines on the (τ,ξ) plane, defined by

$$\frac{d\xi}{d\tau}=-\frac{\tanh\xi}{\tau}-\frac{g\mathcal{E}(\tau)}{p_T\cosh\xi} . \tag{3.37}$$

This equation determines the particle trajectories (characteristic lines) in the (τ,η) space in the presence of the Lorentz force exerted by the time-dependent electric field $\mathcal{E}(\tau)$. Two points (τ,ξ) and (τ',ξ') on the same characteristic line are related by

$$\tau'\sinh\xi'=\tau\sinh\xi-\frac{g}{p_T}\int_\tau^{\tau'}d\tau''\,\tau''\mathcal{E}(\tau'') . \tag{3.38}$$

The kinetic equation can therefore be integrated formally with the initial condition (3.8) as

$$f(\tau,p_T,\xi)=\frac{1}{\tau_c}\int_0^\tau f_{\rm eq}(\tau',p_T,\xi')\exp\left[\frac{1}{\tau_c}(\tau'-\tau)\right]d\tau' +\frac{1}{p_T}\int_0^\tau\frac{S(\tau',p_T,\xi')}{\cosh\xi'}\exp\left[\frac{1}{\tau_c}(\tau'-\tau)\right]d\tau' , \tag{3.39}$$

where ξ' is understood as a function of τ' determined by (3.38). The integral of the source term can be easily performed by inserting (3.7),

$$f(\tau,p_T,\xi)=\frac{1}{\tau_c}\int_0^\tau f_{\rm eq}(\tau',p_T,\xi')\exp\left[\frac{1}{\tau_c}(\tau'-\tau)\right]d\tau' +\sum_i\exp\left[\frac{-\pi p_T^2}{g|\mathcal{E}(\tau_i)|}\right]\exp\left[\frac{1}{\tau_c}(\tau_i-\tau)\right] , \tag{3.40}$$

where the τ_i's are the solutions of

$$\tau\sinh\xi+\frac{g}{p_T}\int_{\tau_i}^\tau\tau''\mathcal{E}(\tau'')d\tau''=0 . \tag{3.41}$$

Note that Eq. (3.41) may have more than one solutions if $\mathcal{E}(\tau)$ does not have a definite sign, but instead oscillates in time (as we will see later, this actually happens when the collision time is large). Physically, this reflects the fact that particles which were created at $\xi=0$ at different points in (τ,p_T) space may arrive at the same point in (τ,p_T,ξ) space simultaneously if the direction of the field has been altered. On the other hand, if the field does not oscillate, particles which were originally created at $\xi=0$ are accelerated always in the same direction. In this case ξ deviates from $\xi=0$ more and more as time elapses and any particle trajectory in (τ,p_T,ξ) space can pass a certain ξ at most once, and therefore there is only one solution to (3.41).

The simplicity of the result (3.40) is deceptive. We emphasize that we have not solved our problem yet. We still need to know the τ dependence of $\mathcal{E}$ and T to actually carry out the τ integral in (3.40) with the condition (3.38) and to solve Eq. (3.41). As we have explained in the previous section, the values of T and $\mathcal{E}$ at a given instant of time are determined by solving (3.20) and (3.22) simultaneously with the kinetic equation. We can use (3.40) to eliminate the distribution functions from (3.20) and (3.22). This yields two coupled integro-differential equations for $T(\tau)$ and $\mathcal{E}(\tau)$. These equations are solved numerically to determine $T(\tau)$ and $\mathcal{E}(\tau)$ for the initial conditions $T(0)=0$ and $\mathcal{E}(0)=\mathcal{E}_0$, and then the result can be used to determine the distribution function from (3.40) finally.

The integral form of the kinetic equation (3.40) becomes particularly simple in the collisionless limit $(\tau_c\to\infty)$,

$$f(\tau,p_T,\xi)=\sum_i\exp\left[\frac{-\pi p_T^2}{g|\mathcal{E}(\tau_i)|}\right] , \tag{3.42}$$

with the τ_i's given by (3.41). Therefore, p_T dependence of the distribution function at given time is determined by that at particle creation at earlier time. The p_L dependence of the distribution function is determined implicitly by that of τ_i. In fact, (3.41) is equivalent at $z=0$ to

$$p_L=\frac{g}{\tau}\int_{\tau_i}^\tau\tau'\mathcal{E}(\tau')d\tau' . \tag{3.43}$$

This equation determines the longitudinal momentum of particles which reside at $z=0$ at time $\tau=t$ taking into account the acceleration by the color field after their creation at earlier times. In the absence of the color field, we always have $p_L=0$ at $z=0$. This is, of course, trivial since we have assumed $v_z=z/t$ at the particle creation, and therefore in the absence of the field acceleration only particles with $p_L=0$ remain at $z=0$. It follows from this result that the p_L distribution is bounded in the absence of collision if the field strength attenuates faster than $1/\tau$ at large τ. We shall see later that this is indeed the case.

Incidentally, we note here that the relation (3.38) can be written as

$$\tau\left[p_T\sinh\xi+\frac{g}{\tau}\int_0^\tau d\tau''\,\mathcal{E}(\tau'')\tau''\right] =\tau'\left[p_T\sinh\xi'+\frac{g}{\tau'}\int_0^{\tau'}d\tau''\,\mathcal{E}(\tau'')\tau''\right] . \tag{3.44}$$

The quantity in the parentheses is nothing but the canonical longitudinal momentum of the particle at $z=0$. To see this choose the gauge

$$A^\mu(x)=(\sinh\eta,0,0,\cosh\eta)a(\tau)\equiv s^\mu a(\tau) , \tag{3.45}$$

so that $a(\tau)$ satisfies $\mathcal{E}(\tau)=a'(\tau)+a(\tau)/\tau$. Then one can show

$$-p_T\sinh\xi-\frac{g}{\tau}\int_0^\tau d\tau''\,\mathcal{E}(\tau'')\tau''=s_\mu(p^\mu-gA^\mu) \equiv\Pi_L . \tag{3.46}$$

This quantity in fact coincides with the canonical longitu-

dinal momentum $\Pi_z \equiv p_z - gA_3$ at $z=0$, where $s^\mu=(0,0,0,1)$. Equation (3.44) implies that $\tau\Pi_L$ is a constant of motion. In other words, the canonical longitudinal momentum Π_z of a particle at $z=0$ decreases monotonically, inversely proportional to time t from its value at particle creation:

$$\Pi_L(\tau)=\frac{\tau_i}{\tau}\Pi_L(\tau_i)=-\frac{\tau_i}{\tau}ga(\tau_i)\ , \tag{3.47}$$

where we have used $\xi_i=0$. We add here, to avoid possible confusion, that we still have to know the time evolution of $f(\tau,p_T,\xi)$ and $\mathcal{E}(\tau)$ to determine $a(\tau_i)$.

It would be useful to compare here our result with that of Bialas and Czyż.[11] They imposed the initial conditions on the distribution function and the field strength at certain early proper time $\tau=\tau_{\rm in}$, and assumed that particle number is conserved afterwards. This is equivalent to assuming that the quarks and antiquarks are created at $\tau=\tau_{\rm in}$ at once by the following source term:

$$S(\tau,p_T,\xi)=\delta(\tau-\tau_{\rm in})\delta(\xi)G(p_T)\ . \tag{3.48}$$

In this case one finds

$$f(\tau,p_T,\xi)=\frac{\tau_{\rm in}}{\tau}\delta(\Pi'_L)G(p_T)\ , \tag{3.49}$$

where the argument of the δ function is

$$\begin{aligned}\Pi'_L &\equiv -p_T\sinh\xi-\frac{g}{\tau}\int_{\tau_{\rm in}}^{\tau}d\tau'\,\tau'\mathcal{E}(\tau')\\ &=\Pi_L-\frac{\tau_{\rm in}}{\tau}\Pi_L^{\rm in}\ .\end{aligned} \tag{3.50}$$

Therefore, in this model the particle longitudinal momentum at later time is uniquely determined and the p_T distribution at $\tau=\tau_{\rm in}$ is maintained throughout the later evolution of the system. In our result (3.42) the longitudinal momentum distribution becomes continuous because of the continuous particle creation and the p_T distribution does not factorize for the same reason.

IV. LINEARIZED COLLISIONLESS BOLTZMANN-VLASOV EQUATION AND THE PLASMA OSCILLATION

One of the most remarkable properties of the collisionless Boltzmann-Vlasov equation, or the Vlasov equation for short, is that it permits the existence of an oscillatory solution, known as the plasma oscillation. Before presenting the numerical results we discuss in this section how such plasma oscillation will show up in our model system in the linear approximation.

The derivation of the plasma oscillation solution usually starts from the linearization of the transport equations with respect to the field strength and the small disturbance in the distribution function around some steady-state solution. We meet two difficulties in applying this method directly to our problem. First, our model kinetic equation contains the particle source term, which is nonlinear in the field strength, and the linearization of the kinetic equation eliminates the source term: Therefore, if we still impose the same initial condition as (3.8) at $\tau=0$ on the distribution function, then we would end up with a trivial result: $f=0$. We shall circumvent this problem by considering the evolution of the system starting from some later time when the field strength has already diminished to some very small value. The second problem is that the solution to our model kinetic equation is nonsteady even in the absence of the field: This is essentially due to the Lorentz-boost-invariant symmetry in the solution. We therefore need to extend the usual perturbation theory analysis to the perturbation with respect to a nonstationary solution.

Suppose the solution of our model kinetic equation is known at some time τ_1 as

$$f(\tau_1,p_T,\xi)=\bar{f}(\tau_1,p_T,-\xi)=F(p_T,\xi),\quad \mathcal{E}(\tau_1)=\mathcal{E}_1\ . \tag{4.1}$$

We may construct an approximate analytic solution for $\mathcal{E}(\tau)$ at later times $\tau>\tau_1$ by treating the effect of the field as small perturbation. To do this we write

$$f(\tau,p_T,\xi)=f_0(\tau,p_T,\xi)+f_1(\tau,p_T,\xi)+O(\mathcal{E}^2)\ , \tag{4.2}$$

$$\bar{f}(\tau,p_T,\xi)=f_0(\tau,p_T,-\xi)+f_1(\tau,p_T,-\xi)+O(\mathcal{E}^2)\ , \tag{4.3}$$

where it is understood that the f_1 is the order of $g\mathcal{E}$ and the unperturbed boost-invariant distribution function f_0 does not depend on the field strength. This implies that f_0 and f_1 satisfy the following linearized transport equations:

$$\frac{\partial f_0}{\partial\tau}-\frac{\tanh\xi}{\tau}\frac{\partial f_0}{\partial\xi}=0\ , \tag{4.4}$$

$$g\int d\Gamma\, p_T\sinh\xi f_0=0\ , \tag{4.5}$$

and

$$\frac{\partial f_1}{\partial\tau}-\frac{\tanh\xi}{\tau}\frac{\partial f_1}{\partial\xi}=\frac{g\mathcal{E}}{p_T\cosh\xi}\frac{\partial f_0}{\partial\xi}\ , \tag{4.6}$$

$$-\frac{d\mathcal{E}}{d\tau}=2g\int d\Gamma\, p_T\sinh\xi f_1\ . \tag{4.7}$$

The initial conditions of $f_0(\tau,p_T,\xi)$ and $f_1(\tau,p_T,\xi)$ at $\tau=\tau_1$, which are compatible with (4.1) and (4.5), are

$$\begin{aligned}f_0(\tau_1,p_T,\xi)&=F_0(p_T,\xi)\\ &=\tfrac{1}{2}[F(p_T,\xi)+F(p_T,-\xi)]\ ,\end{aligned} \tag{4.8}$$

$$\begin{aligned}f_1(\tau_1,p_T,\xi)&=F_1(p_T,\xi)\\ &=\tfrac{1}{2}[F(p_T,\xi)-F(p_T,-\xi)]\ .\end{aligned} \tag{4.9}$$

The solution of the unperturbed kinetic equation (4.4) for the initial condition (4.8) can be found immediately by the method of characteristics:

$$\begin{aligned}f_0(\tau,p_T,\xi)&=F_0(p_T,\sinh^{-1}(\tau\sinh\xi/\tau_1))\\ &\equiv\mathcal{F}_0(p_T,\tau\sinh\xi)\ .\end{aligned} \tag{4.10}$$

Note that $f_0(\tau,p_T,\xi)$ is an even function of ξ due to (4.8)

and therefore Eq. (4.5) is automatically satisfied. We insert this result into (4.6). Integration of (4.6) along the characteristic lines $\tau\sinh\xi=$const yields

$$f_1(\tau,p_T,\xi)=\frac{g}{p_T}\left[\frac{\partial\mathcal{F}_0(p_T,z)}{\partial z}\right]_{z=\tau\sinh\xi}\int_{\tau_1}^{\tau}d\tau'\,\tau'\mathcal{E}(\tau')+\mathcal{F}_1(p_T,\tau\sinh\xi)\ , \tag{4.11}$$

where the function $\mathcal{F}_1(p_T,z)$ is defined by

$$\mathcal{F}_1(p_T,z)=F_1(p_T,\sinh^{-1}(z/\tau_1))\ . \tag{4.12}$$

This function is odd in z since $F_1(p_T,\xi)$ is an odd function of ξ by construction. It then follows immediately from (4.11) that $f_1(\tau,p_T,\xi)$ is an odd function of ξ.

The right-hand side of the linearized field equation (4.7) can now be modified using (4.11) as

$$2g\int d\Gamma\,p_T\sinh\xi f_1=2g\int d\Gamma\,p_T\sinh\xi\frac{g}{p_T}\left[\frac{\partial\mathcal{F}_0(p_T,z)}{\partial z}\right]_{z=\tau\sinh\xi}\int_{\tau_1}^{\tau}d\tau'\,\tau'\mathcal{E}(\tau')+2g\int d\Gamma\,p_T\sinh\xi\mathcal{F}_1(p_T,\tau\sinh\xi)$$
$$=\frac{2g^2\gamma}{(2\pi)^2\tau}\int_0^\infty dp_T\,p_T\int_{-\infty}^{\infty}dz\frac{z}{(\tau^2+z^2)^{1/2}}\frac{\partial\mathcal{F}_0}{\partial z}\int_{\tau_1}^{\tau}d\tau'\,\tau'\mathcal{E}(\tau')+\frac{2g\gamma}{(2\pi)^2\tau}\int_0^\infty dp_T\,p_T^2\int_{-\infty}^{\infty}dz\frac{z\mathcal{F}_1}{(\tau^2+z^2)^{1/2}}\ , \tag{4.13}$$

where, in deriving the last line, we have made the change in the integration variable by $z=\tau\sinh\xi$. We now assume that the functions $\mathcal{F}_0(p_T,z)$ and $\mathcal{F}_1(p_T,z)$ are both well localized in z around $z=0$. Then we can approximate the phase-space integrals in (4.13) by replacing $(\tau^2+z^2)^{1/2}$ in the integrand by τ. This gives

$$2g\int d\Gamma\,p_T\sinh\xi f_1=\frac{c_0}{\tau^2}\int_{\tau_1}^{\tau}d\tau'\,\tau'\mathcal{E}(\tau')+\frac{c_1}{\tau^2}\ , \tag{4.14}$$

where the constants c_0 and c_1 are defined by

$$c_0=\frac{2g^2\gamma}{(2\pi)^2}\int_0^\infty dp_T\,p_T\int_{-\infty}^{\infty}dz\,\mathcal{F}_0(p_T,z)\ , \tag{4.15}$$

$$c_1=\frac{2g\gamma}{(2\pi)^2}\int_0^\infty dp_T\,p_T^2\int_{-\infty}^{\infty}dz\,z\mathcal{F}_1(p_T,z)\ , \tag{4.16}$$

respectively, or we can write them explicitly in terms of the distribution function at $\tau=\tau_1$:

$$c_0=2g^2\tau_1\int d\Gamma\cosh\xi f(\tau_1,p_T,\xi)\ , \tag{4.17}$$

$$c_1=2g\tau_1^2\int d\Gamma\,p_T\sinh\xi\cosh\xi f(\tau_1,p_T,\xi)\ . \tag{4.18}$$

We note that the constant c_0 is always positive.

The linearized field equation now takes the form

$$\frac{c_0}{\tau^2}\int_{\tau_1}^{\tau}d\tau'\,\tau'\mathcal{E}(\tau')+\frac{c_1}{\tau^2}=-\frac{d\mathcal{E}}{d\tau}\ . \tag{4.19}$$

We can convert this integro-differential equation to a simple second-order differential equation:

$$\frac{d^2\mathcal{E}}{d\tau^2}+\frac{2}{\tau}\frac{d\mathcal{E}}{d\tau}+c_0\frac{\mathcal{E}}{\tau}=0\ , \tag{4.20}$$

with the initial conditions

$$\mathcal{E}(\tau_1)=\mathcal{E}_1,\quad\left[\frac{d\mathcal{E}}{d\tau}\right]_{\tau=\tau_1}=-\frac{c_1}{\tau_1^2}\ . \tag{4.21}$$

Since the constant c_0 is positive, the solution of this linearized field equation becomes oscillatory. It is given approximately by

$$\mathcal{E}(\tau)=\frac{\beta}{\tau^{3/4}}\sin(\Omega\tau^{1/2}+\delta)\ , \tag{4.22}$$

where we have omitted the terms involving the higher power of $1/\tau$. Three parameters Ω, β, and δ are given in terms of c_0, c_1, and $\mathcal{E}_1$ by

$$\Omega=2c_0^{1/2}\ , \tag{4.23}$$

$$\beta=\tau_1^{3/4}\left[\mathcal{E}_1^2+\frac{c_1^2}{c_0\tau_1^3}\right]^{1/2}\ , \tag{4.24}$$

$$\tan(\Omega\tau_1^{1/2}+\delta)=-\frac{\tau_1^{3/2}c_0^{1/2}\mathcal{E}_1}{c_1}\ , \tag{4.25}$$

in the approximation retaining the leading-power term of $1/\tau_1$.

The constant Ω has the dimension of (time)$^{-1/2}$ and is not the usual oscillation frequency. The oscillation frequency ω can be found by writing $\tau=\tau_1+\delta\tau$ and expanding the above result in terms of $\delta\tau/\tau_1$. This yields

$$\mathcal{E}(\tau)\simeq\mathcal{E}_{\rm os}\sin(\omega\delta\tau+\delta')\ , \tag{4.26}$$

with

$$\omega=\frac{\Omega}{2\tau_1^{1/2}}=\left[\frac{c_0}{\tau_1}\right]^{1/2}\ , \tag{4.27}$$

$$\mathcal{E}_{\rm os}=\frac{\beta}{\tau_1^{3/4}}=\left[\mathcal{E}_1^2+\frac{c_1^2}{c_0\tau_1^3}\right]^{1/2}\ , \tag{4.28}$$

$$\delta'=\Omega\tau_1^{1/2}+\delta\ . \tag{4.29}$$

We can show using (4.17) that the square of the frequency is related to the integral of the distribution function at $\tau=\tau_1$,

$$\omega^2=2g^2\int d\Gamma\cosh\xi f(\tau_1,p_T,\xi)\ . \tag{4.30}$$

It is interesting to note that if we replace $f(\tau_1,p_T,\xi)$ by the local equilibrium distribution function (3.12), then we find

$$\omega^2 = 2g^2 \int d\Gamma \cosh\xi f_{\rm eq}(\tau_1, p_T, \xi)$$
$$= \frac{g^2\gamma\pi}{24} T^2 , \tag{4.31}$$

which differs from the well-known result for the plasma frequency, $\omega_{\rm pl}^2 = (g^2\gamma/12)T^2$, by the factor of $\pi/2$. The origin of this difference can be traced back to the factor $\cosh\xi$ in the integrand, which is absent in the ordinary plasma oscillation. This factor has arisen because of the nonstatic Lorentz-boost-invariant symmetry in the solution. In the actual collisionless evolution of the system, the form of the distribution function is always very different from the equilibrium one. In such cases we can write the formula (4.30) using the scaling properties of the distribution function found in the preceding section as

$$\omega^2 = 2g^2\gamma(g\mathcal{E}_0) \int d\hat{\Gamma} \cosh\xi \hat{f}(\hat{\tau}_1, \hat{p}_T, \xi) . \tag{4.32}$$

Comparing (4.32) to (4.31), we see that in the nonequilibrium collisionless evolution the quantity $g\mathcal{E}_0 \int d\hat{\Gamma} \cosh\xi \hat{f}$ plays a role similar to the square of the temperature at time $\tau = \tau_1$.

We also find using (4.18) that the amplitude of the plasma oscillation can be written as

$$\mathcal{E}_{\rm os} = \left[\mathcal{E}_1^2 + \frac{\mathcal{J}^2}{\omega^2} \right]^{1/2} , \tag{4.33}$$

where

$$\mathcal{J} = 2g \int d\Gamma\, p_T \sinh\xi \cosh\xi f(\tau_1, p_T, \xi) \tag{4.34}$$

measures the strength of the color current in the plasma at time τ_1. Unless both $\mathcal{E}_1$ and $\mathcal{J}$ vanish in our initial conditions, which is very unlikely, $\mathcal{E}_{\rm os}$ is finite. We may thus conclude from this result that the plasma oscillation almost always appears spontaneously in the collisionless evolution of our system. [The condition $\omega\tau_1 \gg 1$ must be satisfied for a well-defined plasma oscillation to develop. According to (4.30), this condition is equivalent to

$$2g^2\gamma\hat{\tau}_1^2 \int d\hat{\Gamma} \cosh\xi \hat{f}(\hat{\tau}_1, \hat{p}_T, \xi) \gg 1 , \tag{4.35}$$

which is always satisfied if $\hat{\tau}_1$ is sufficiently large.]

V. NUMERICAL RESULTS AND DISCUSSIONS

Our numerical calculation has been performed in two steps. First, the integral form (3.41) and (3.42) of the kinetic equation was solved self-consistently with the temperature equation (3.20) and the field equation (3.22). Next, the resultant distribution function is used to calculate the dilepton spectrum using the formulas (2.17)–(2.20). Owing to the scale-invariant properties of the solutions with respect to the initial conditions as discussed in Sec. III B, we have only two free parameters in our calculations: the effective coupling strength $g^2\gamma$ and the scaled collision time $\hat{\tau}_c$. Throughout our calculations we set $\gamma = 12$, which corresponds to a two-flavor quark-antiquark plasma. We chose two different values of the coupling constant $g = 2,5$, which correspond to $g^2\gamma = 48,300$, respectively, and cover the range for $\alpha_s = g^2/(4\pi)$ from 0.31 to 2.0.

A. The plasma oscillation

We first show the time evolution of the field intensity and the proper energy density in the collisionless limit ($\hat{\tau}_c = \infty$) in Figs. 2 and 3, respectively. They show that the plasma oscillation is indeed excited spontaneously in the system, as expected from our more general analysis in the previous section. In the beginning the field intensity decreases monotonically, converting its energy to the proper energy density and flow energy of the plasma. The field intensity eventually vanishes, but continues to decrease for a while with opposite sign. This overshooting is caused by the conduction current generated in the plasma, which polarizes the color charge in the plasma. This decrease of the field is eventually halted by the restoring force exerted by the electrostatic force between two polarized charges, and then the field oscillation follows.

The frequency and amplitude of the plasma oscillation depend on $g^2\gamma$. In the case of strong coupling ($g = 5$), both the amplitude and period of the plasma oscillation are small, the amplitude being so small that it is hardly visible in these figures, while in the weak coupling case ($g = 2$) the oscillation is so prominent that one can see the oscillation of the proper energy density of the plasma out of phase with the field oscillation. This may first look contradictory to what one would naively expect from the formula (4.30), which suggests that the frequency of the plasma oscillation is proportional to the coupling constant.

To understand this behavior, we must first of all recall that here we have used the scaled time $\hat{\tau} = \tau(g\mathcal{E}_0)^{1/2}$ in these figures; thus, in the physical time scale, the results for smaller coupling would be prolonged in the time direction. We replotted, therefore, in Fig. 4, the same results against the rescaled time $g^{1/2}\hat{\tau}$. It now appears that

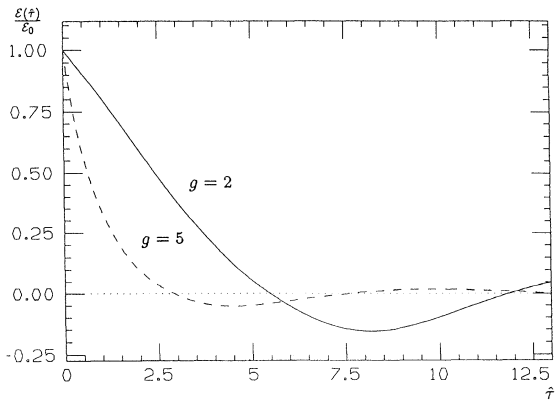

FIG. 2. Time evolution of the field intensity $\mathcal{E}$, scaled by the initial field strength $\mathcal{E}_0$ in the collisionless limit. Solid and dashed curves are for $g = 2$ and 5, respectively. The proper time τ is scaled as $\hat{\tau} = \tau\sqrt{g\mathcal{E}_0}$.

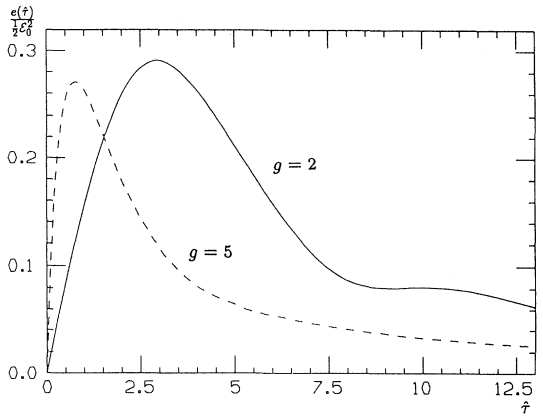

FIG. 3. Time evolution of the proper energy density of matter e, scaled by the initial field energy density $\mathcal{E}_0^2/2$ in the collisionless limit.

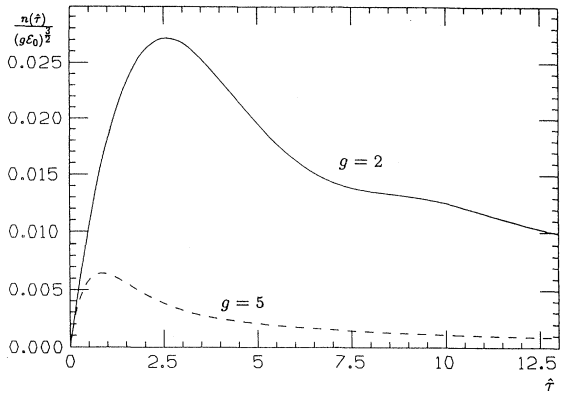

FIG. 5. Time evolution of the proper particle density n scaled by $(g\mathcal{E}_0)^{3/2}$.

the oscillation frequencies are almost the same for both cases. Further insight can be obtained by looking at the time evolution of the proper quark density $n(\tau) = \int d\Gamma\, u_u p^\mu f(x;p)$ as shown in Fig. 5. For a larger coupling the field initially decays faster, and because of the boost-invariant expansion, the initial field energy is converted faster into plasma flow energy; this results in a lower plasma density. This is the reason why the amplitude of the plasma oscillation is smaller for a larger coupling constant. The weak g dependence of the plasma frequency may be explained as a result of the effective cancellation of the factor g^2 in the formula for the plasma frequency (4.32) with the $g^2\gamma$ dependence of the quark density.

We plot in Fig. 6 a snapshot of the charge-density distribution $\rho(t,z)=j^0_{\rm cond}(t,z)$ at $\tau/\tau_0=2$ for $g=2$. Note that the charge density is antisymmetric by the space reflection, $\rho(t,z)=-\rho(t,-z)$, and by this symmetry the plasma is always neutral at $z=0$: This also implies that the proper charge density $j(\tau)=u_\mu j^\mu_{\rm cond}$ must always vanish. The charge density becomes large in the vicinity of two light-cone edges $t=\pm z$, where the Lorentz-contracted color-charged nuclei reside (it vanishes right at the light cone), decreases monotonically for a while as we go away from each edge toward the interior, and then oscillates. It may first seem that the apparent increase of the charge density near the edges is caused by the Lorentz-contraction factor $\gamma=[1-(z/t)^2]^{-1/2}=t/\tau$, which diverges at the light cone where $\tau=0$. There is yet another effect of special relativity near the edges, i.e., the time dilatation: since the time evolution is delayed near the edges and there should not be much quarks and antiquarks produced yet which are needed to generate the current in the system. In fact, one can show that the charge density actually vanishes in the very vicinity of the edges in proportion to τ. The oscillation of the charge density is the manifestation of the plasma oscillation. The amplitude of the oscillation decreases since the plasma has been diluted more in the interior where the proper time has elapsed more.

The distribution functions obtained by this calculation are shown in Fig. 7 where the time evolution of the

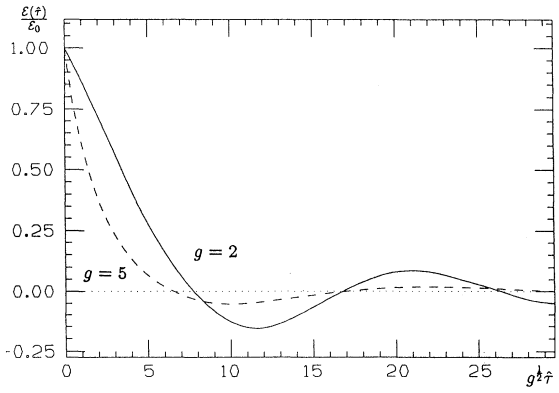

FIG. 4. Same as Fig. 2 plotted against rescaled proper time $g^{1/2}\hat{\tau}$.

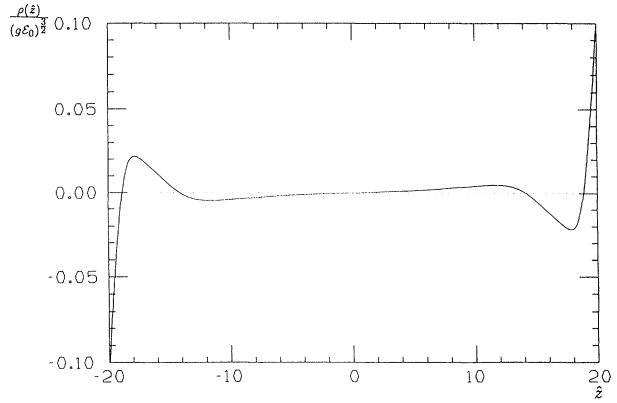

FIG. 6. Snapshot of the charge-density distribution j_0 at $\hat{\tau}=20.67$ for $g=2$. The z coordinate is scaled as $\hat{z}=z\sqrt{g\mathcal{E}_0}$.

longitudinal-momentum distribution of the quarks seen at $z=0$ is plotted. In this plot we chose three different values for the transverse momentum, $\hat{p}_T=0.112$, 0.282, and 0.452, and set $g=2$. Note that the particles with finite longitudinal momentum which are seen at $z=0$ have originally been produced earlier ($t=t_0$) at some different place $z_0\neq 0$ with the longitudinal momentum given by $p_L=p_T\sinh\eta_0=p_T z_0/\tau_0$ and have traveled along a curved trajectory in the Minkowski space, being accelerated gradually by the background field; in the absence of acceleration by the background field, these particles would travel a straight line at a constant longitudinal velocity $v_z=p_L/E=z_0/t_0$ and never show up at $z=0$. It is seen that the field acceleration stretches out the longitudinal-momentum distribution of particles at $z=0$ gradually until the field flips its sign (this happens in this case at $\hat{\tau}\simeq 6$ as seen from Fig. 2); after this time, particles are accelerated backward until the direction of the field changes again. Note that the sharp edges in the longitudinal-momentum distribution have arisen as a result of our assumption that a particle is always created with zero longitudinal momentum at $z=0$. It is interesting to note that the location of the sharp edges of the distribution function in the (τ,p_L) plane does not depend on the transverse momentum. This is simply due to the fact that the rate of the change of the longitudinal momentum is determined by the Lorentz force $g\mathcal{E}(\tau)$, which does not depend on the transverse momentum of the particle, as we have shown explicitly in (3.44). The maximum of the longitudinal momentum of particles occurs in this case at $\hat{p}_L\simeq 0.86$, namely, $p_L\simeq 0.86\sqrt{g\mathcal{E}_0}$. This value, however, depends on the time evolution of the field and, hence, on the value of the coupling constant g. For larger coupling constant the Lorentz force acting on the particles becomes bigger, but the field decays faster; the latter effect wins over the former since $\Delta p_L\sim g\mathcal{E}_0\tau_0\propto g^{-3/2}\gamma^{-1}\mathcal{E}_0^{1/2}$ from (3.35). Therefore, the maximum value of the longitudinal momentum becomes smaller for larger coupling

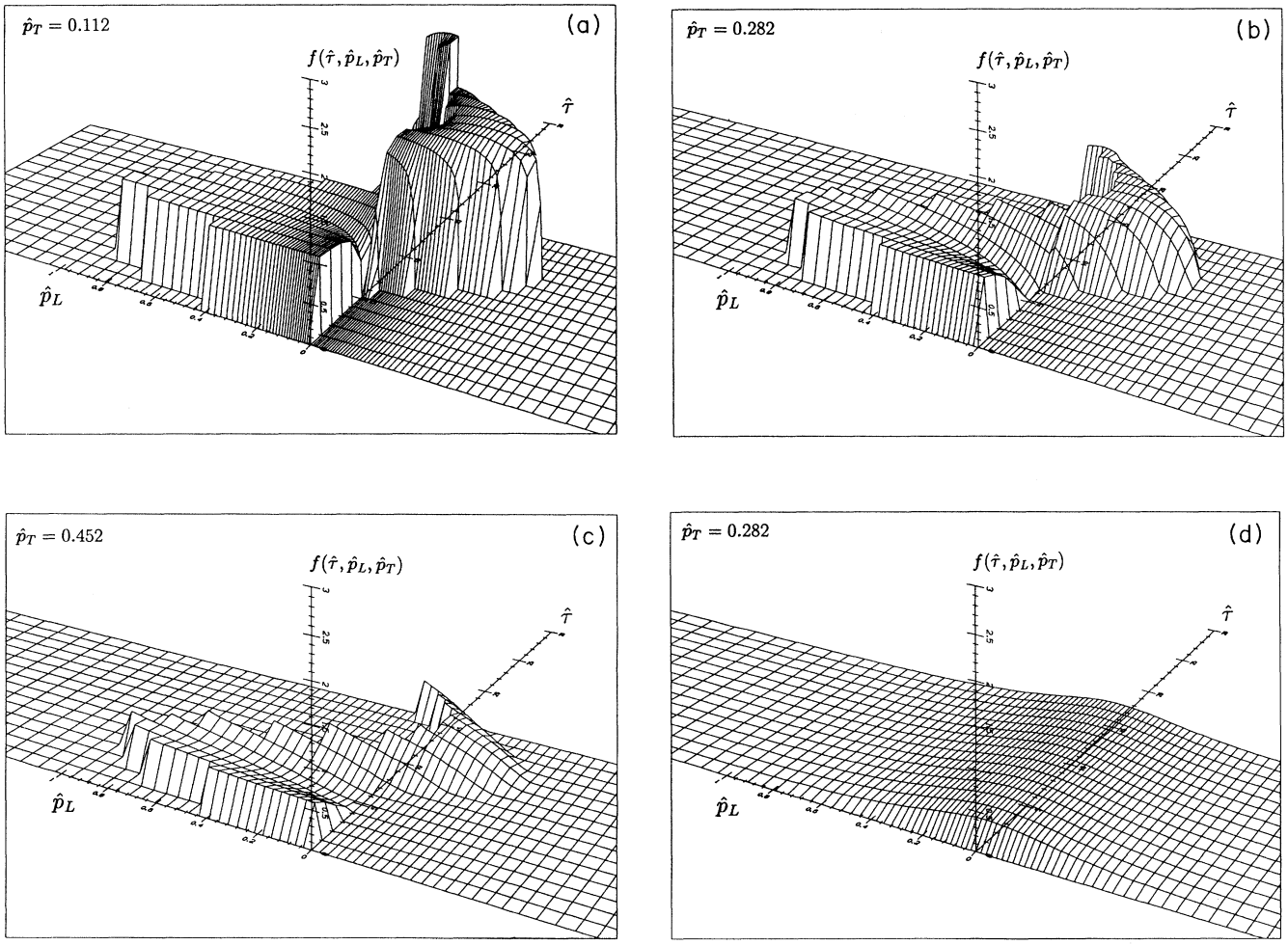

FIG. 7. Time evolution of the longitudinal-momentum distribution of particles for $g=2$ in the collisionless limit at (a) $\hat{p}_T=p_T/(g\mathcal{E}_0)^{1/2}=0.112$, (b) $\hat{p}_T=0.282$, and (c) $\hat{p}_T=0.452$. The result in the hydrodynamic limit is also plotted for (d) $\hat{p}_T=0.282$.

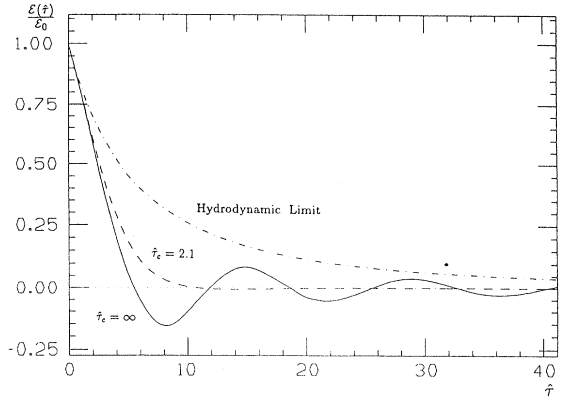

FIG. 8. Comparison of time evolution of the field intensity for three different values of the collision time $\hat{\tau}_c = \tau_c (g\mathcal{E}_0)^{1/2}$: Solid line is for $\hat{\tau}_c = \infty$ (the collisionless limit); dashed line for $\hat{\tau}_c = 2.1$; dot-dashed line for $\hat{\tau}_c = 0$ (the hydrodynamic limit). All computed for $g = 2$.

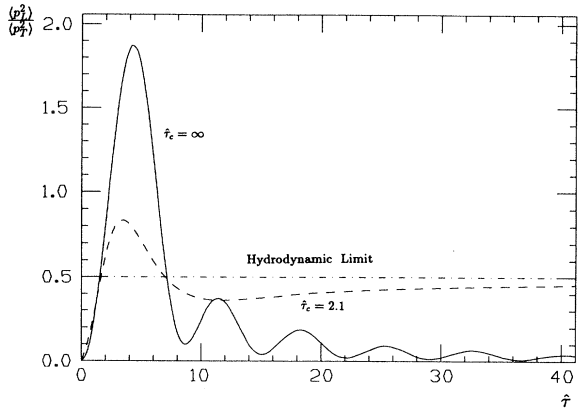

FIG. 10. Time evolution of the ratio of the average longitudinal momentum and the average transverse momentum. The solid curve is for the collisionless limit, the dashed curve for $\hat{\tau}_c = 2.1$ and the dot-dashed curve is for the hydrodynamic limit. All computed for $g = 2$.

constant. The height of the distribution is determined by the rate of particle creation at the point where the particle was created and hence depends on the transverse momentum. It is seen that at small p_T the particle piles up at small p_L as the time elapses. This is caused by the particle creation at later times when the field strength is weakened and, therefore, happens only at small transverse momenta since high-p_T-momentum particles are produced only at early times when the field strength is large enough so that the production rate for such particles is not to be suppressed by the Gaussian form of the source term. At large p_T the distribution function has a peak at the edge where the particles created at the early time (when the field is strong) reside. It is expected, however, that this interesting nontrivial behavior of the distribution function will be smoothed out in the presence of the collision. The time evolution of the distribution function in the extreme local equilibrium situation is shown in Fig. 7(d). In this case the distribution function decreases monotonically for all value of p_T.

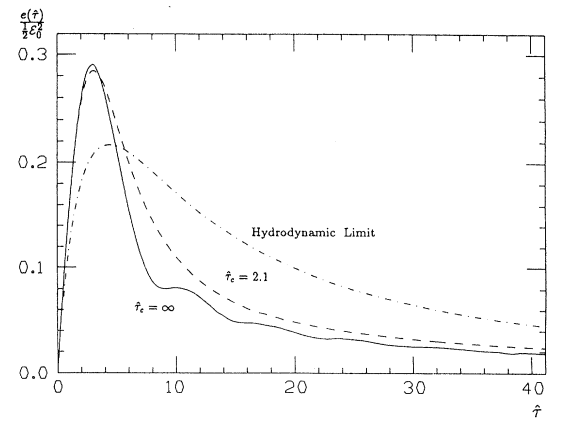

FIG. 9. Same as Fig. 8 for the proper energy density of matter.

In Figs. 8–10 we study the effect of the collisions comparing three cases at $g = 2$: (i) the collisionless limit ($\hat{\tau}_c = \infty$), (ii) the hydrodynamic limit ($\hat{\tau}_c = 0$), and (iii) the case with finite collision time ($\hat{\tau}_c = 2.1$). In the last case we have chosen a rather small value for the collision time compared with the time scale of the plasma oscillation, which is $\simeq 10$. Nonetheless, the results with the finite collision time differ significantly from those in the hydrodynamic limit as far as the field intensity and plasma energy density are concerned. They look, rather, more like the average behavior of the collisionless limit where the oscillatory feature which is characteristic of the collisionless limit is smeared out. It appears, however, the result of the case (iii) is very similar to the hydrodynamic limit in the momentum distribution of particles. To show this we plot the ratio of the average of squared longitudinal momentum and the average of squared transverse momentum, $\langle p_L^2 \rangle / \langle p_T^2 \rangle$ at $z = 0$, in Fig. 10. This quantity is always 0.5 in any proper frame in the hydrodynamic limit. Note that in the collisionless limit this quantity eventually reaches zero, since all particles with finite longitudinal velocity will go away from $z = 0$. Figure 10 shows, however, that this ratio finally reaches 0.5 in the case of finite collision time. This is so for any value of τ_c because for $\tau \gg \tau_c$ the hydrodynamic approximation should become valid.

B. Dilepton spectrum

We now turn to the discussion of the dilepton spectrum. We have seen that in the collisionless limit the evolution of the distribution function shows some prominent features which are absent in the case of (local) equilibrium as assumed in the hydrodynamic calculations. We study how these nontrivial features will be reflected in the spectrum of dilepton pairs emitted from such a nonequilibrium quark-gluon plasma.

We concentrate here on two extreme limits, i.e., the collisionless and hydrodynamic limits. In the following

calculations we use $g=2$. To make our result concrete, we set the physical scale by measuring the initial field energy density $\mathcal{E}_0^2/2$ in a physical unit (GeV/fm^3). Also, we introduce a new parameter e_f, the "final" proper energy density, which specifies a cutoff time τ_f in the integration over the proper time in (2.16) by $e(\tau_f)=e_f$. This parameter may be considered as the proper energy density at which the quark phase ceases to exist and the transition to the confining hadronic phase starts. Here we only calculate the contribution from the plasma phase and neglect dileptons from all other sources, e.g., Drell-Yan processes, mixed phase, hadron gas phase, etc. It may be expected that contributions from the mixed and hadronic phases would not be significant at sufficiently high energies. The parameters τ_f and e_f are related to the energy per unit rapidity at the transition time by

$$\frac{dE}{dy}=\tau_f e_f S \ , \tag{5.1}$$

where S is the transverse cross section of the volume occupied by the plasma, which may be given by $S=\pi R^2$ for a central collision of nuclei of radius R. This quantity may be compared with the observed transverse energy deposited in the central rapidity region. To compare the result obtained in the collisionless limit to that in the hydrodynamic limit, we chose the same value for e_f, but adjusted the initial field intensity so that it gives the same value for dE/dy, when calculated excluding gluon excitations, as in the collisionless case. The numerical values for these parameters used in our calculation are listed in Table I.

Also shown in the table are the values for the number of particles per unit rapidity at the transition time calculated by

$$\frac{dN}{dy}=2\tau_f n_f S \ , \tag{5.2}$$

where n_f is the proper density of quarks at $\tau=\tau_f$. In the hydrodynamic limit the number of the excitations in the system is related to the entropy, and this may be related directly to the observed multiplicity of the particle since the entropy is conserved even during the hadronization transition. In the nonequilibrium evolution, however, the relation between the number of excitations in the quark phase and the observed particle multiplicity is not so clear. We conjecture that dE/dy is less affected than dN/dy by the details of the hadronization transition and the later evolution of the system. Thus we adopt dE/dy rather than dN/dy to adjust the initial conditions of two extreme cases so that they correspond to similar final observable conditions.

The result for the dilepton spectrum obtained in the collisionless limit is shown in Fig. 11. The two figures correspond to the two different values of the initial field energy: $\mathcal{E}_0^2/2=10$ GeV/fm^3 [Fig. 11(a)] and $\mathcal{E}_0^2/2=20$ GeV/fm^3 [Fig. 11(b)]. In this calculation the transverse cross section was set as $S=\pi R^2=140$ fm^2, corresponding to a U+U central collision. We have chosen two different values for q_T of dilepton: Solid lines in each figure are at $q_T=0$ GeV and dashed lines at $q_T=1$ GeV. According to formula (2.15), the dilepton spectrum depends only on the variable M_T at $M \gg m_l$ in the case of one-dimensional scaling hydrodynamic expansion, but this scaling is violated in the case of nonequilibrium evolution. It is seen that this violation of M_T scaling is prominent only at small M_T (<2 GeV), but not so significant at large M_T. In these figures we also present results for two different values of e_f: Upper lines in each case are for $e_f=1$ GeV/fm^3 and the lower lines for $e_f=2$ GeV/fm^3. It is seen that the spectrum is not sensitive to the choice of this parameter in the large-M_T region ($M_T>2$ GeV). This indicates that dileptons with large M_T are created only at the early stage.

In Fig. 12 the collisionless and hydrodynamic limits are compared. The solid and dashed lines correspond to $q_T=0$ and 1 GeV, respectively, with $\mathcal{E}_0^2/2=10$ GeV/fm^3, $e_f=1$ GeV/fm^3, and $g=2$ in the collisionless limit. The dot-dashed lines represent the dilepton creation rate from the thermalized plasma with the initial conditions specified as we described earlier. It is seen that in the collisionless limit the rate is enhanced at small M_T and is suppressed much at large M_T compared with the hydrodynamic limit. We found that this tendency persists for all parameter sets in the absence of collision. Also shown are the expected yields for the Drell-Yan pairs at pp center-of-mass energy $\sqrt{s}=200$ GeV scaled to UU central collisions assuming a simple factorization of the nuclear mass dependence. [The transverse-momentum dependence of the Drell-Yan pairs is calculated from the formula (5.7.14) in Ref. 34 for the perturbative QCD estimate of gluon emission (infrared singularities being regulated by "Sudakov form factor") by taking a convolution with the Gaussian primordial transverse-momentum distribution of primary partons.[35]] It may be expected naively that from the preequilibrium quark-gluon plasma rather high-energy dileptons are produced and that the contribution of those is seen significantly in an intermediate region, which lies between the low-mass region which

TABLE I. Values of the parameters used in the numerical calculation ($\mathcal{E}_0'$ is the field strength which would give the same dE/dy in the hydordynamic limit. See text for definitions of other parameters).

$\frac{1}{2}\mathcal{E}_0^2$ (GeV/fm^3)	e_f (GeV/fm^3)	τ_f (fm)	$\frac{dE}{dy}$ (GeV)	$\frac{dN}{dy}$	$\frac{1}{2}\mathcal{E}_0'^2$ (GeV/fm^3)
10	2	1.2	320	550	9.3
	1	1.6	230	580	4.8
20	2	1.4	380	810	9.6
	1	2.7	380	1060	6.5

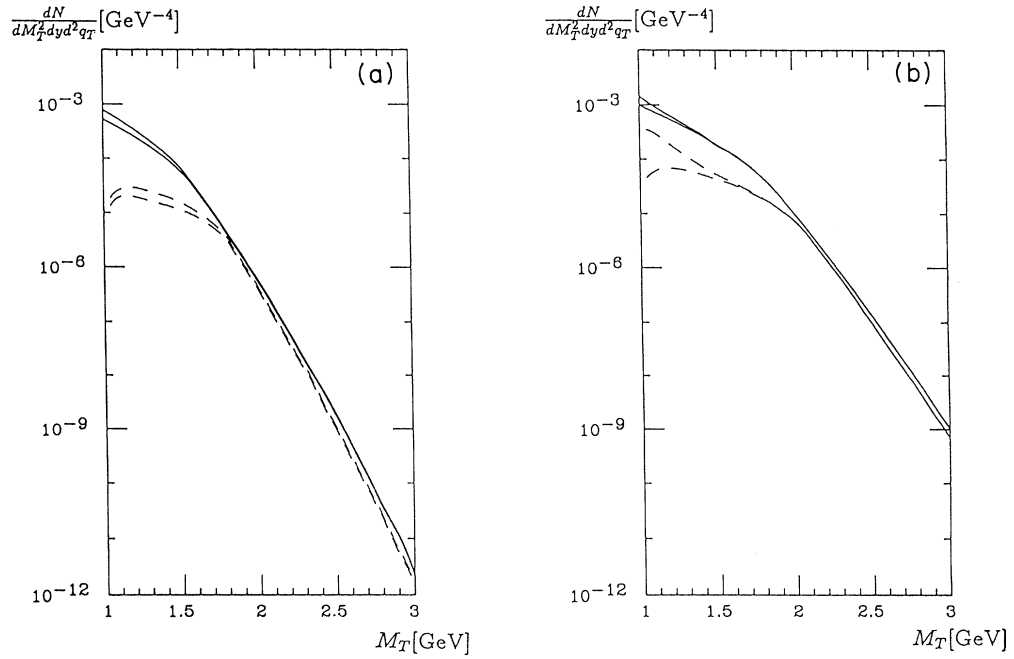

FIG. 11. (a) Dilepton yield calculated by using the distribution function for collisionless evolution is plotted against the transverse dilepton mass. The physical scales are set by choosing $\mathcal{E}_0^2/2=10$ GeV/fm^3 and $g=2$. Solid lines are for $q_T=0$ and dashed lines for $q_T=1$ GeV. The upper curves were computed with the final (cutoff) proper energy density $e_f=1$ GeV/fm^3 and lower curves with $e_f=2$ GeV/fm^3. (b) Same as (a) but with higher initial energy density $\mathcal{E}_0^2/2=20$ GeV/fm^3.

is dominated by the thermal pairs and the high-mass region dominated by the Drell-Yan pairs. Our results, however, do not show such an intermediate behavior.

To understand this behavior qualitatively, it is instructive to approximate the distribution function by the following simplified form similar to that used in Ref. 10 [see (3.50)]:

$$f(\tau,p_T,\xi)\sim\frac{1}{\tau}\exp\left[-\frac{\pi p_T^2}{g\mathcal{E}_0}\right]\delta(p_T\sinh\xi+P(\tau))\ , \tag{5.3}$$

where

$$P(\tau)=\frac{g}{\tau}\int_0^\tau \tau''\mathcal{E}(\tau'')d\tau'' \tag{5.4}$$

is the longitudinal momentum of particles at $z=0$, where $p_T\sinh\xi=-p_L$. This may be a good approximation at large p_T since, as we have shown, the distribution function at time τ has a sharp peak at $p_L=P(\tau)$, where the particles created at $\tau=0$ reside. With this approximation three integrals in the formula for the differential dilepton yield (2.16) and (2.17) can be performed analytically, owing to the two δ functions and the Gaussian form of the p_T dependence,[10] and one obtains

$$\frac{dN}{dM_T^2\,dy\,d^2q_T}\sim\frac{1}{M^2}\exp\left[-\frac{\pi q_T^2}{2g\mathcal{E}_0}\right]\int\frac{d\tau}{\tau}\exp\left[-\left[2+\frac{q_T^2}{M^2}\right]\frac{\pi[M^2-4P^2(\tau)]}{4g\mathcal{E}_0}\right]I_0\left[\frac{\pi q_T^2[M^2-4P^2(\tau)]}{4M^2g\mathcal{E}_0}\right]\ , \tag{5.5}$$

where $I_0(x)$ is the modified Bessel function of the first kind and the integration is taken over the region of τ, which satisfies the kinematical condition $M\geq 2P(\tau)$.

This approximate formula for the dilepton spectrum has a derivative singularity at

$$M_T=(4P_{\max}^2+q_T^2)^{1/2}\equiv M_{T_s}\ , \tag{5.6}$$

where $P_{\max}$ is the maximum value of the longitudinal momentum given by (5.4). This derivitive singularity arises as a result of the kinematic condition $M\geq 2P(\tau)$, which is always satisfied when M_T becomes greater than M_{T_s} since $M^2-4P_{\max}^2=M_T^2-M_{T_s}^2$. At large transverse masses ($M_T>M_{T_s}$), the spectrum is essentially Gaussian. On the other hand, at lower transverse masses ($M_T<M_{T_s}$), the dilepton yield becomes suppressed compared with the extrapolation of this Gaussian because of

the limitation of the integral over τ by the condition $M \geq 2P(\tau)$, which arises when $M_T < M_{T_s}$. At lower transverse mass this constraint becomes more severe and this makes the spectrum a shoulderlike shape. The slope of yield grows infinitely as the transverse mass approaches to M_{T_s} from below. This singular behavior at M_{T_s} has appeared as a result of the δ-function approximation of the longitudinal-momentum distribution and is therefore smoothed out in the actual numerical calculation. Yet we can still see the remnant of this derivative singularity in our numerical result. For instance, with the parameters used for Fig. 11(a), $\mathcal{E}_0^2/2 = 10$ GeV/fm^3 and $g=2$, we find $P_{\max} = 0.77$ GeV, which gives $M_{T_s} = 1.55$ and 1.84 GeV for $q_T = 0$ and 1 GeV, respectively; these values of M_{T_s} in fact coincide with the values of M_T around which the spectrum changes its shape in Fig. 11(a). We found that $P_{\max}$ cannot exceed 1.5 GeV within a reasonable range of the parameters: $1 \leq g \leq 5$ and $dE/dy = 300-400$ GeV for U+U collisions. Thus our model does not predict the intermediate behavior in the dilepton spectrum between the thermal exponential shape and the Drell-Yan power-law shape in the region where two lines intercept.

This analysis also gives an intuitive understanding of the origin of M_T-scaling violation in the low-M_T region. The suppression of the yield at large q_T and small M_T is due to the kinematical reason that the condition $M^2 = M_T^2 - q_T^2 \geq 4P^2(\tau)$ severely constrains the phase space of the available quarks and antiquarks which can produce dilepton. We note that direction of the scaling violation in our calculation is opposite to that caused by the transverse flow.[6]

The dilepton spectrum from a thermalized plasma which undergoes a cylindrical boost-invariant expansion with the four-flow-velocity

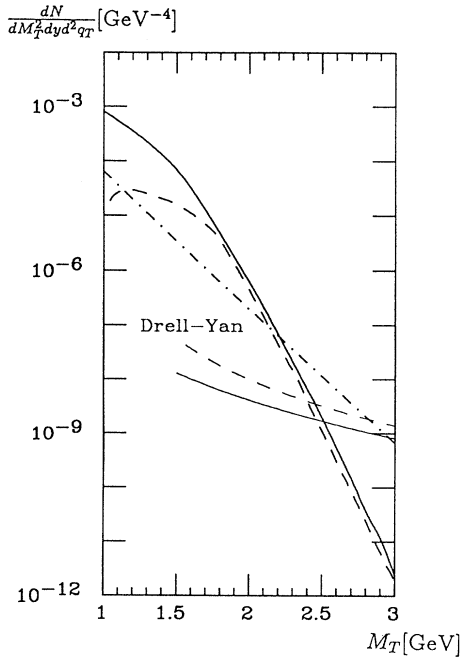

FIG. 12. Comparison of the dilepton spectrum for the case of collisionless evolution (solid and dashed lines) and the case of hydrodynamic (thermal) evolution (dot-dashed line). The parameters for the collisionless case are the same as in Fig. 11(a). The initial conditions of the hydrodynamic evolution were chosen so that they give the same value for dE/dy (excluding gluon excitations) at the cutoff time. Note that the spectrum in the hydrodynamic limit does not depend on the transverse momentum q_T of the dilepton. Two curves below the sign "Drell-Yan" are a prediction of the dilepton yield due to the Drell-Yan mechanism at $q_T = 0$ (solid line) and at $q_T = 1$ GeV (dashed line) calculated by perturbative QCD (Refs. 34 and 35).

$$u^\mu = (\cosh\alpha \cosh\eta,\ \sinh\alpha \cos\varphi,\ \sinh\alpha \sin\varphi,\ \cosh\alpha \sinh\eta) \tag{5.7}$$

is given by

$$\frac{dN}{dM_T^2\, dy\, d^2q_T} \sim 4\pi \int d\tau\, \tau \int d\rho\, \rho I_0(q_T \sinh\alpha(\tau,\rho)/T(\tau,\rho)) K_0(M_T \cosh\alpha(\tau,\rho)/T(\tau,\rho)) , \tag{5.8}$$

where $I_0(x)$ and $K_0(x)$ are the modified Bessel function of the first and second kind, respectively. Since $I_0(x)$ is positive definite and monotonously increasing function of x for $x > 0$, this formula predicts that in the presence of the transverse flow $\alpha > 0$ the yield increases with q_T at a fixed M_T. Since matter is cooled (and perhaps already hadronized) when the transverse expansion becomes significant, this hydrodynamic M_T-scaling violation is expected to be significant also at relatively small M or M_T. Similar effect would arise even in the case of nonequilibrium evolution of the plasma if one includes the effect of transverse expansion, which we expect, however, is not significant in the plasma phase since the lifetime of the plasma is 1–2 fm in the present estimate, which is much shorter than the transverse size of the system.

VI. SUMMARY AND CONCLUSION

We have studied dilepton emission from a quark-gluon plasma which might be produced in the course of an ultrarelativistic nucleus-nucleus collision based on the semiclassical kinetic theory. In this formalism we are able to relax the condition of local thermodynamic equilibrium on the one-body distribution function of the quarks and antiquarks, a strong condition which has been assumed in most of the earlier works. We applied this method to the flux-tube model for ultrarelativistic nucleus-nucleus collisions. This model assumes that a quark-gluon plasma is created by the pair creation from strong color electric field which spans between two color-charged nuclei. We have computed the nonequilibrium evolution of the quark distribution function by

solving the Boltzmann-Vlasov equation which couples to the field equation for the background color field for a one-dimensional boost-invariant evolution.

It was shown that in the collisionless limit, a collective plasma oscillation is excited spontaneously in the system and the evolution of the quark distribution function differs considerably from that in the local thermodynamic equilibrium. As we have examined analytically in the linearization approximation to the Boltzmann-Vlasov equation, the excitation of such collective excitation is inevitable in the boost-invariant collisionless evolution. The amplitude of this nonequilibrium plasma oscillation attenuates gradually because of the Lorentz-boost-invariant longitudinal expansion. This collective behavior of the plasma is a characteristic of collisionless evolution and the collisions between plasma constituents, which drive the system toward local thermodynamic equilibrium and thus lead to hydrodynamic expansion, work to suppress the plasma oscillation.

We used the resultant nonequilibrium quark and antiquark distribution functions to compute the dilepton spectrum and compared the result with that obtained by assuming local thermodynamic equilibrium. Contrary to our most naive expectation, our model predicts that the dilepton emission from nonequilibrium plasma is suppressed in the high-mass region and, instead, enhanced in the low-mass region in comparison with the spectrum obtained from equilibrium plasma.

The suppression in the high-mass region is essentially due to the Gaussian transverse-momentum distribution in the particle source term used in our model kinetic equation. We note that this Gaussian shape of the transverse-momentum distribution is a consequence of the Schwinger mechanism of the particle creation in a constant uniform-color electric field. We have assumed, however, a strong correlation between the longitudinal momentum and the space-time position for particle creation in determining the unknown longitudinal-momentum dependence of the source term, as done in the previous works[21–23] so that the spreads in the longitudinal-momentum distribution at each space-time point arises only from the acceleration of the particle by the field after its creation. Our result indicates that the Gaussian shape of the transverse-momentum distribution in the source term dominates the high-mass tail of the dilepton spectrum in the collisionless limit, which diminishes faster than the exponential falloff of the spectrum from equilibrium plasma. The longitudinal acceleration of the quarks just after their creation by the remaining strong color field is not quite significant enough to alter this behavior at the high-mass region, although it is essential for the excitation of color plasma oscillation. It remains to be seen, however, whether or not a more microscopic treatment of the particle creation based on a fully quantum-mechanical formulation of the problem alters our result at the high-mass region.

It was shown that the effect of the collective plasma oscillation appears as an enhancement of the yield in the relatively low-mass region. These pairs are produced by the annihilation of low-energy quarks and antiquarks while they oscillate out of phase collectively. The role of the color plasma oscillation here is to provide an intense and extended source of low-energy quark-antiquark flux for the incoherent process of $q\bar{q}$ pair annihilation into lepton pair. Although our model for nonequilibrium plasma evolution still lacks in the description of later hadronization stage,[36] we do not anticipate a significant change in these behaviors: The pairs created at the later stages of matter evolution would only contribute to enhancement in the low-mass regions.

We would like to note here that a large enhancement of the low-mass dilepton pairs has actually been observed in high-energy pp collisions,[37] and this effect has been interpreted by several authors[38–40] as due to the annihilation of low-energy partons (quarks and antiquarks) produced by the collision. Our physical picture is somewhat similar in spirit to that of these authors. We would like to emphasize, however, that the effect we have studied in this paper is a genuine collective phenomenon which involves large degrees of freedom to participate in the process coherently in a large space-time volume. In this sense it should be regarded as a phenomenon unique to nucleus-nucleus collisions, although some precursory effect may exist even in pp or p-nucleus collisions.

We finally note that one of the characteristic behaviors of the dilepton spectrum predicted by our model, namely, the violation of the M_T scaling in the low-mass region, can be tested experimentally.

ACKNOWLEDGMENT

It is our pleasure to thank Arthur Kerman and Koichi Yazaki for critical discussions. M.A. thanks John Negele and Laboratory for Nuclear Science for arranging financial support which enabled him to do this research and colleagues for a lot of hospitality extended to him during his stay at MIT. This work was supported in part by funds provided by the U.S. Department of Energy (DOE) under Contract No. DE-AC02-76ER03069.

APPENDIX

In this appendix we derive the formula (2.17) for the dilepton creation rate.

We start with the following expression for W given by (2.13) for the boost-invariant one-particle distribution functions $f(\tau,p_T,\xi)$ and $\bar{f}(\tau,p_T,\xi)$, which we assume are the same for all species:

$$W(\tau,M,q_T,\eta-y)=\frac{RM^2}{4\pi^2}\int\frac{d^3p_1}{E_1}\int\frac{d^3p_2}{E_2}f(\tau,p_{T_1},\xi_1)\bar{f}(\tau,p_{T_2},\xi_2)\delta^4(p_1+p_2-q)\ , \tag{A1}$$

where $\xi_1=\eta-y_1$ and $\xi_2=\eta-y_2$. The p_2 integral in (A1) is carried out easily to give

$$W(\tau,M,q_T,\eta-y)=\frac{RM^2}{4\pi^2}\int dp_{T_1}\,dy_1\,d\varphi\frac{p_{T_1}}{E_2}f(\tau,p_{T_1},\xi_1)\bar{f}(\tau,p_{T_2},\xi_2)\delta(|\mathbf{p}_1|+|\mathbf{q}-\mathbf{p}_1|-q_0)\ , \tag{A2}$$

where we have used $d^3p_1/E_1=p_{T_1}\,dp_{T_1}\,dy_1\,d\varphi$.

Since we know that the final result of W is invariant by the boost in the beam direction, we have freedom to choose any Lorentz frame, which is transformed to each other by such a boost, to calculate this quantity. It is convenient to work in the frame where the longitudinal momentum of the pair vanishes, $q_z=0$, or equivalently the rapidity of the pair vanishes, $y=0$. We set the frame so that the direction of the pair momentum coincides with x direction:

$$q^\mu=(M_T,q_T,0,0)\ . \tag{A3}$$

In this frame we write

$$p_1^\mu=(p_{T_1}\cosh y_1,\ p_{T_1}\cos\varphi_1,\ p_{T_1}\sin\varphi_1,\ p_{T_1}\sinh y_1)\ . \tag{A4}$$

Then we find

$$|\mathbf{q}-\mathbf{p}_1|=(q_T^2+p_{T_1}^2\cosh^2 y_1-2p_{T_1}q_T\cos\varphi_1)^{1/2}\ . \tag{A5}$$

The argument of the δ function, $|\mathbf{p}_1|+|\mathbf{q}-\mathbf{p}_1|-q_0$, therefore vanishes at

$$\varphi=\pm\arcsin\left[\frac{[p_{T_1}^2q_T^2-(p_{T_1}M_T\cosh y_1-M^2/2)^2]^{1/2}}{p_{T_1}q_T}\right]$$
$$\equiv\pm\varphi_0\ , \tag{A6}$$

for p_{T_1} such that $p_-\le p_{T_1}\le p_+$, where

$$p_\pm=\frac{M^2/2}{M_T\cosh y_1\mp q_T}\ . \tag{A7}$$

Performing the φ integral in (A2), we finally find

$$W(\tau,M,q_T,\eta)=\frac{RM^2}{2\pi^2}\int_{-\infty}^{\infty}d\xi_1\int_{p_-}^{p_+}dp_{T_1}\frac{p_{T_1}f(\tau,p_{T_1},\xi_1)\bar{f}(\tau,p_{T_2},\xi_2)}{[p_{T_1}^2q_T^2-(p_{T_1}M_T\cosh y_1-M^2/2)^2]^{1/2}}\ , \tag{A8}$$

where the arguments of the antiquark distribution are related to the integration variables by the energy-momentum conservation, $p_2^\mu=q^\mu-p_1^\mu$, which immediately gives

$$p_{T_2}=[M_T^2-2M_Tp_{T_1}\cosh(\eta-\xi_1)+p_{T_1}^2]^{1/2}\ . \tag{A9}$$

To find the relation between ξ_2 and integration variables, we define a vector $s^\mu=(\sinh\eta,0,0,\cosh\eta)$ and calculate $s_\mu p_1^\mu+s_\mu p_2^\mu=s_\mu q^\mu$, which yields

$$\sinh\xi_2=\frac{M_T\sinh\eta-p_{T_1}\sinh\xi_1}{p_{T_2}}\ . \tag{A10}$$

Formula (A8) coincides with (2.17), except that we have replaced $\eta\to\xi$ to recover the manifest boost invariance.

In the limit of $q_T\to0$, where $p_{T_1}=p_{T_2}$ and $y_1=-y_2$, the p_T integral in (A8) can be carried out analytically, and one finds a more compact formula

$$W(\tau,M,0,\xi)=\frac{RM^2}{4\pi}\int_{-\infty}^{\infty}d\xi_1\frac{1}{\cosh^2(\xi-\xi_1)}f(\tau,p_T,\xi_1)\bar{f}(\tau,p_T,\xi_2)\ , \tag{A11}$$

where $p_T=M/[2\cosh(\eta-\xi_1)]$ and $\xi_2=2\eta-\xi_1$.

---

*Present address.

[1]E. V. Shuryak, Yad. Fiz. **28**, 796 (1978) [Sov. J. Nucl. Phys. **28**, 408 (1978)]; Phys. Lett. **78B**, 150 (1978).

[2]K. Kajantie and H. Miettinen, Z. Phys. C **9**, 341 (1981); K. Kajantie and P. V. Ruuskanen, Phys. Lett. **121B**, 352 (1983).

[3]G. Domokos and J. Goldman, Phys. Rev. D **23**, 203 (1981); G. Domokos, *ibid.* **28**, 123 (1983).

[4]L. D. McLerran and T. Toimela, Phys. Rev. D **31**, 545 (1985).

[5]R. Hwa and K. Kajantie, Phys. Rev. D **32**, 1109 (1985).

[6]K. Kajantie, M. Kataja, L. McLerran, and P. V. Ruuskanen,

Phys. Rev. D **34**, 811 (1986).
[7]K. Kajantie, J. Kapusta, L. McLerran, and A. Mekjian, Phys. Rev. D **34**, 2746 (1986).
[8]T. Matsui and H. Satz, Phys. Lett. B **178**, 416 (1986).
[9]J. D. Bjorken, Phys. Rev. D **27**, 140 (1983).
[10]A. Białas and J.-P. Blaizot, Phys. Rev. D **32**, 2954 (1985).
[11]A. Białas and W. Czyż, Phys. Rev. D **30**, 2371 (1984).
[12]H. Ehtamo, J. Lindfors, and L. McLerran, Z. Phys. C **18**, 341 (1983).
[13]T. S. Biro, H. B. Nielsen, and J. Knoll, Nucl. Phys. **B245**, 449 (1984).
[14]A. Białas and W. Czyż, Phys. Rev. D **31**, 198 (1985).
[15]A. K. Kerman, T. Matsui, and B. Svetitsky, Phys. Rev. Lett. **56**, 219 (1986).
[16]J. Schwinger, Phys. Rev. **82**, 664 (1951).
[17]E. Brezin and C. Itzykson, Phys. Rev. D **2**, 1191 (1970).
[18]C. Martin and D. Vautherin, Phys. Rev. D **40**, 1667 (1989).
[19]F. Low, Phys. Rev. D **12**, 163 (1975).
[20]S. Nussinov, Phys. Rev. Lett. **34**, 1286 (1975).
[21]K. Kajantie and T. Matsui, Phys. Lett. **164B**, 373 (1985).
[22]G. Gatoff, A. K. Kerman, and T. Matsui, Phys. Rev. D **36**, 114 (1987).
[23]A. Białas, W. Czyż, A. Dyrek, and W. Florkowski, Nucl. Phys. **B296**, 611 (1988); A. Białas and W. Czyż, Act. Phys. Pol. B **17**, 635 (1986).
[24]U. Heinz, Phys. Rev. Lett. **51**, 351 (1983); Ann. Phys. (N.Y.) **161**, 48 (1985).
[25]H.-Th. Elze, M. Gyulassy, and D. Vasak, Phys. Lett. B **177**, 402 (1986).
[26]B. Banerjee, R. S. Bhalerao, and V. Ravishankar, Phys. Lett. B **224**, 16 (1989).
[27]G. Baym, Phys. Lett. **138B**, 18 (1984).
[28]J. D. Bjorken, in *Current Induced Reactions,* proceedings of the International Summer School on Theoretical Particle Physics, Hamburg, 1975, edited by J. G. Körner, G. Kramer, and D. Schildnecht (Lecture Notes in Physics, Vol. 56) (Springer, New York, 1976), p. 93.
[29]A. Casher, H. Neuberger, and S. Nussinov, Phys. Rev. D **20**, 179 (1979).
[30]B. Andersson, G. Gustafson, and T. Sjöstrand, Z. Phys. C **6**, 235 (1980).
[31]N. K. Glendenning and T. Matsui, Phys. Rev. D **28**, 2890 (1983).
[32]M. Gyulassy and A. Iwazaki, Phys. Lett. **165B**, 157 (1985).
[33]S. R. de Groot, W. A. van Leeuwen, and Ch. G. van Weert, *Relativistic Kinetic Theory* (North-Holland, Amsterdam, 1980).
[34]R. D. Field, *Applications of Perturbative QCD* (Addison-Wesley, Reading, MA, 1989).
[35]M. Asakawa, Ph.D. thesis (submitted to University of Tokyo), 1991.
[36]M. Kataja and T. Matsui, Ann. Phys. (N.Y.) **192**, 383 (1989).
[37]K. J. Anderson *et al.*, Phys. Rev. Lett. **37**, 799 (1976); for the recent data, see T. Åkesson *et al.*, Phys. Lett. B **192**, 463 (1987), and the references therein.
[38]J. D. Bjorken and H. Weisberg, Phys. Rev. D **13**, 1405 (1976).
[39]V. Černý, P. Lichard, and J. Pišút, Phys. Lett. **70B**, 61 (1977).
[40]L. van Hove, Ann. Phys. (N.Y.) **192**, 66 (1989).